Acoustic Analysis of Musical Pillars of Vitthala Temple, Hampi

by

LAKSHMIPRIYA V. K.
201211031

A Thesis Submitted in Partial Fulfilment of the Requirements for the Degree of

MASTER OF TECHNOLOGY
in
INFORMATION AND COMMUNICATION TECHNOLOGY
to

DHIRUBHAI AMBANI INSTITUTE OF INFORMATION AND COMMUNICATION TECHNOLOGY



August, 2014

Declaration

I hereby declare that

i) the thesis comprises of my original work towards the degree of Master of Technology in Information and Communication Technology at Dhirubhai Ambani Institute of Information and Communication Technology and has not been submitted elsewhere for a degree,

ii) due acknowledgment has been made in the text to all the reference material used.

Lakshmipriya V. K.

Certificate

This is to certify that the thesis work entitled, "Acoustic Analysis of Musical Pillars of Vitthala Temple, Hampi", has been carried out by Lakshmipriya V. K. for the degree of Master of Technology in Information and Communication Technology at *Dhirubhai Ambani Institute of Information and Communication Technology* under my supervision.

Dr. Hemant A. Patil
Thesis Supervisor

Acknowledgments

First of all, I would like to express my sincere gratitude and appreciation to my thesis supervisor Dr. Hemant A. Patil. He has been of tremendous help at all stages of the thesis and has motivated me to work hard. I would also like to thank my thesis subject expert Prof. Aditya Tatu for his valuable comments and suggestions which helped in the progress of this thesis. At different stages, he has helped me identify the limitations of the work and suggested ways to improve it. This work is a part of the project, "Immersive Navigation for Walk-through Application", which is a constituent part of the consortium project, *viz.*, India Digital Heritage (IDH)-Hampi sponsored by Department of Science and Technology (DST), Govt. of India. I thank Prof. M.V. Joshi, who is a principal investigator of the project (with Dr. Hemant Patil as Co-PI), and also DST for their support in carrying out this research. I am very much grateful to DA-IICT resource centre, for providing me with enough technical references whenever needed. The staff were really helpful in acquiring certain publications which were not available otherwise.

Special thanks to Dr. Anish Kumar and Dr. Jayakumar at Indira Gandhi Centre for Atomic Research, Kalpakkam, Tamilnadu, for providing the relevant data from musical pillars. In addition, they devoted their precious time for discussion regarding this project and suggested many directions in which the work can continue. I express my gratitude to Dr. Sharada Srinivasan, National Institute of Advanced Sciences, Bangalore, for providing sound data from pillars for the study.

I thank all my friends who has supported me, technically and otherwise, through this entire process. Finally, I express my gratitude towards my family for encouraging and supporting me in all my pursuits.

Contents

Abstract vi

List of Principal Symbols and Acronyms viii

List of Tables ix

List of Figures x

1 Introduction 1
- 1.1 Vitthala Temple at Hampi . . . 1
- 1.2 Problem Description . . . 2
- 1.3 Outline of the Thesis . . . 3
- 1.4 Literature Survey . . . 4
  - 1.4.1 Study of Musical Pillars . . . 4
  - 1.4.2 Beam Modelling . . . 5
  - 1.4.3 Linear Prediction . . . 5
  - 1.4.4 Digital Waveguide Modelling . . . 5
- 1.5 Contributions of this thesis . . . 6
- 1.6 Chapter Summary . . . 6

2 Dimensional and Spectral Analysis of Pillars and the Sounds Produced 7
- 2.1 Introduction . . . 7
- 2.2 Dimensional Measurements . . . 7
- 2.3 Non-Destructive Testing . . . 8
- 2.4 The Veena Pillar . . . 9
- 2.5 Analysis of Sound from Musical Pillars . . . 11
  - 2.5.1 Spectral Analysis . . . 12
- 2.6 Chapter Summary . . . 15

3 Vibration Analysis of Musical Columns using Beam Modelling 16
- 3.1 Introduction . . . 16

3.2 Modelling a Transversely Vibrating Beam . . . 16
3.3 Beam Equilibrium Equations . . . 17
3.3.1 The Elastic Flexure Formula . . . 19
3.4 Euler-Bernoulli Model for Musical Columns . . . 20
3.4.1 Solution of Euler-Bernoulli Equation . . . 20
3.4.2 Boundary Conditions . . . 22
3.5 Timoshenko Beam Model for Musical Columns . . . 24
3.5.1 Solution of Timoshenko Beam Equation . . . 25
3.5.2 Boundary Conditions . . . 28
3.6 Constants in the Solution . . . 30
3.7 Calculating Flexural Frequency . . . 32
3.8 Chapter Summary . . . 33

4 Linear Prediction (LP) Analysis of Musical Pillars 34
4.1 Introduction . . . 34
4.2 Linear Prediction . . . 34
4.3 Finding Optimal LPCs . . . 35
4.3.1 The Levinson-Durbin Algorithm . . . 37
4.4 Estimating Prediction Order . . . 38
4.5 The LP Spectrum . . . 38
4.6 Estimating Area Function using the Concatenated Tube Model . . . 40
4.7 Experimental Results . . . 41
4.8 Chapter Summary . . . 43

5 Sound Synthesis using Digital Waveguide Modelling 44
5.1 Introduction . . . 44
5.2 Synthesis of Musical Sounds . . . 44
5.3 The Ideal *1-D* Wave Equation . . . 46
5.3.1 Travelling Wave Solution . . . 46
5.3.2 Sampling the Travelling Waves . . . 46
5.3.3 Incorporating Losses . . . 47
5.3.4 Consolidating Losses . . . 48
5.3.5 Frequency-dependent Losses . . . 49
5.3.6 Initial Wave Pattern . . . 49
5.3.7 Rigid Terminations . . . 50
5.4 Towards *3-D* modelling . . . 50
5.4.1 Lossless Scattering Junctions . . . 50
5.5 Simulation . . . 53

5.5.1 *1-D* model . . . 53
5.5.2 *2-D* model . . . 54
5.5.3 *3-D* model . . . 54
5.6 Chapter Summary . . . 55

6 Conclusions and Future Work **56**
6.1 Conclusions from the Thesis Work . . . 56
6.2 Future Research Directions . . . 57
6.2.1 Acoustics of Musical Pillars . . . 57
6.2.2 Waveguide Modelling . . . 58

References **59**

Appendix A Basic Definitions from Mechanics **62**
A.1 Elasticity . . . 62
A.2 Young's Modulus and Hooke's Law . . . 62
A.3 Shear in Beams . . . 62
A.4 Bending Moment in Beams . . . 63
A.5 Radius of Gyration . . . 63
A.6 Poisson's Ratio . . . 63
A.7 Moment of Inertia . . . 63

Appendix B Important MATLAB Codes **64**
B.1 LP analysis . . . 64
B.2 *1-D* DWG . . . 65
B.3 *2-D* DWG . . . 65

Abstract

This thesis is a systematic investigation on the acoustics of musical pillars of Vitthala temple at Hampi, India. The columns of different pillars produce sounds of different musical instruments (in particular, instruments used in Indian classical music) when struck by a finger. The earlier works in this area constituted a detailed dimensional and spectral analysis of these musical columns. The use of beam theories to model the columns and calculate the flexural frequencies was also suggested before. In this thesis, the performances of two major beam theories, *viz*., Euler-Bernoulli beam theory and Timoshenko beam theory, are compared based on the calculated flexural frequencies. The Euler-Bernoulli model gives better performance despite the fact that it is the simplest beam model and does not consider *shear* and *rotation* effects of beam bending. The concept of linear prediction (LP) from speech processing is applied onto the columns of musical pillars. The LP spectrum obtained matches closely with the spectrum of sound from the pillar. The concatenated tube model is also used to estimate the varying area function of the columns. Furthermore, an attempt for synthesis of sound from musical pillars is presented using the digital waveguide model. Eventhough the synthesized sound is audibly similar to the pillar's sound, the model needs many improvements to match its spectral characteristics with that of the sound from the musical pillar.

List of Principal Symbols and Acronyms

x	Position along the length of the beam
t	Time
y	Deviation/displacement from the rest position
y'	Derivative of y with respect to position x
$\dot{y}$	Derivative of y with respect to time t
θ	Slope of the deflection curve
ψ	Bending angle
ω	Angular frequency
D	Diameter of the beam/musical column
l	Length of the beam/musical column
A	Area of cross-section of the beam/musical column
V_L	Ultrasonic wave velocity through the musical column
E	Young's modulus of the material of the beam/musical column
G	Shear modulus of the material of the beam/musical column
k'	Shear correction factor for the cross-section
ρ	Mass density of the material of the beam/musical column
I	Area moment of inertia
κ	Radius of gyration
k	Wave number
K	String tension

A_i, B_i, C_i Constants which change values according to the context

DWG Digital Waveguide

NDT Non-Destructive testing

LTI Linear Time-Invariant

LP Linear Prediction

a_i Linear Prediction Coefficients

$s(n)$ Actual signal in LP analysis

$\hat{s}(n)$ Signal predicted using LP

P Linear prediction order

$X(z)$ Z-transform of sequence $x(n)$

$n - D$ n-dimensional

FIR Finite Impulse Response

List of Tables

2.1 Dimensions of the Veena pillar 11
2.2 Frequencies of actual and pillar sound. 13
2.3 Pillar dimensions 14

3.1 First four roots of the frequency equation. 23
3.2 Properties of granite, Source: [17] 31
3.3 Comparison of frequencies from two beam models 32

4.1 Comparison of frequencies from LP analysis with that from pillar. . 42

List of Figures

1.1 Vitthala temple 2
1.2 The flow of thesis. 3

2.1 Arrangement of pillars in the Mahamandapam 8
2.2 A Saraswati Veena and its parts. 10
2.3 Three different views of the Veena pillar. 10
2.4 Typical plots for sound from pillar. 11
2.5 Plot of bell-like sound from pillar. 12
2.6 Plot of actual temple bell sound, sound source: [29]. 13

3.1 Elementwise analysis of beams. 18
3.2 A beam undergoing bending. 19
3.3 Musical column clamped at both ends. 22
3.4 The first four mode-shapes of the beam using Euler-Bernoulli model 24
3.5 Plots of $det(M)$ *vs.* ω for columns of Veena pillar. 33

4.1 The concatenated tube model of vocal tract. Adapted from [20]. . . 40
4.2 LP analysis for a column of Veena pillar. 41
4.3 The sound from a column of Veena pillar used for LP analysis. . . . 42
4.4 Estimated area function for two values of prediction order. 42

5.1 Ideal waveguide model 47
5.2 Lossy waveguide model 48
5.3 Consolidating losses 48
5.4 Initial wave pattern 49
5.5 A scattering junction 50
5.6 Major *2-D* mesh structures. Adapted from [26]. 52
5.7 Sound synthesized using *1-D* DWG. 53
5.8 Sound synthesized using *2-D* DWG 54
5.9 Velocity profile of the mesh at different time instants in order. . . . 54
5.10 Sound synthesized using *3-D* DWG 55

CHAPTER 1
Introduction

Acoustics is a very old branch of science that deals with wave propagation in different mediums. The study of vibrations and sound constitutes an important component of acoustics. The term *acoustic* itself has the meaning *for hearing or audible* . The field of acoustics can be dated back to 6^{th} century BC when Pythagoras studied the harmonic properties of musical sounds [4]. It has many branches like musical acoustics, architectural acoustics, speech acoustics, ultrasonics, underwater acoustics, vibration and dynamics, etc.

In this thesis, various aspects of acoustics, especially musical acoustics, are studied and are applied for a specific problem. Musical acoustics is concerned with the physics behind music and musical instruments. Frequency analysis, harmonicity of musical sounds, computer analysis of musical structures and synthesis of musical sounds are some areas of study in musical acoustics [4]. Study of vibration and dynamics of physical systems also plays an important role in this thesis.

This chapter gives an idea about the problem under study and its importance. In addition, this chapter discusses the important published works done in this area which were referred while doing this work.

1.1 Vitthala Temple at Hampi

The village of Hampi is located in the Bellary district of Karnataka, on the southern bank of the river Tungabhadra. This small village was once the imperial capital of the historic Vijayanagara empire. The magnificent architecture of the buildings of Hampi, which are ruins of the ancient city, attracts tourists from both India and abroad. One of the important landmarks of the city and the most magnificent of the religious edifices there, is the *Vitthala temple*. The temple's history can be traced back to AD *1422-46* [1]. The main attraction of the temple is the Mahamandapam or great stage, which has several pillars producing audible sound when

struck by a finger. The sound produced by these pillars are similar to the sound produced by various musical instruments. The Bahamani invaders attacked and burnt the temple in the 15^{th} century, which caused irreparable damage to many of the pillars. Out of a total of *56* pillars in the Mahamandapam, many are now damaged completely or partially [1].



Figure 1.1: The Vitthala temple at Hampi. Adapted from [3].

1.2 Problem Description

This thesis is a detailed and systematic study of the acoustics of musical pillars of the Vitthala temple at Hampi. The *11* most popular pillars which produce sounds of different musical instruments are considered for the study. In particular, the data from the pillars producing bell and Veena sounds were used for experiments and simulations. The pillars, like the other structures of the temple, are made of *granite* stone [2]. Each pillar corresponds to a musical instrument and has several musical columns in it which produces different tones of that instrument. The differences in the sounds produced by the pillars can be attributed to the differences in the size and shape of the pillars. A thorough dimensional analysis is done previously on these pillars [2], which is used extensively in the current study. In addition, a spectral analysis of the various sounds is done.

The thesis is mainly divided into three parts, *viz.*, frequency analysis of pillars using beam modelling, linear prediction analysis and synthesis of sound from pillar. In frequency analysis, the musical columns are modelled using beam modelling techniques and the theoretical frequency of vibration of the columns are found. This is then compared with the measured frequencies of the sounds from musical columns. For this purpose, two beam modelling theories are used, which

are classical/Euler-Bernoulli beam theory and the Timoshenko beam theory. The pros and cons of both these theories are also discussed in the context of current study.

Linear prediction (LP) analysis and concatenated tube model which is used in speech processing is extended to the study of pillars, mapping the vocal tract to the columns of the musical pillars.

The method used for synthesis of sounds is digital waveguide modelling which is an acoustic model. This method comes under the category of physical modelling and is widely used in modelling musical instruments. The model is applied onto the musical columns to generate the sound from it artificially, using the dimensions and material properties of the pillar. The results of the synthesis are also analysed in detail.

1.3 Outline of the Thesis

The thesis is systematically organized into several chapters to aid coherent reading. Each chapter deals with one specific issue in the thesis and discusses it in detail with relevant facts and figures. Figure 1.2 shows the way chapters of the thesis progress.

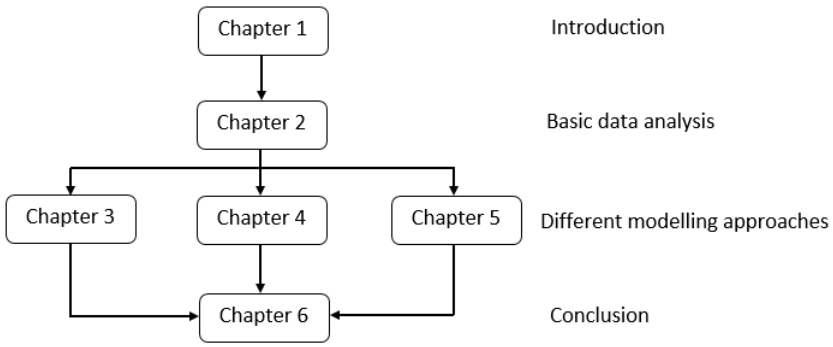


Figure 1.2: The flow of thesis.

In chapter 2, the detailed dimensional analysis of the musical pillars of the Vitthala temple is presented. The average dimensions of columns of *11* pillars as well as exact dimensions of one particular pillar, i.e., the pillar producing the sound of Veena are given. Then, the discussion moves onto the spectral analysis of sounds from pillars. A comparison of sound from a pillar with the actual sound of the corresponding musical instrument is done.

Chapter 3 includes one of the important parts of this study. The theory of Beam modelling is discussed in detail with the help of several derivations, figures

and tables. Starting from the basics of beam bending, it covers two complex beam modelling techniques which are Euler-Bernoulli model and Timoshenko model. Solutions of these models are also given for the particular case of Veena pillar and the results are compared.

Chapter 4 explores the usage of much known Linear Prediction (LP) in the case of musical pillars. This method which is widely used in speech processing applications, is applied onto the musical columns to analyse the LP spectrum and group delay spectrum. The concatenated tube model for vocal tract from speech literature is also used here to find the area function of the musical columns.

Another major component of the thesis is digital waveguide modelling, which is explained in chapter 5. It discusses everything from mathematical equations governing the wave motion, to a complete digital model considering various aspects of the system. It explores one-dimensional, two-dimensional and three-dimensional waveguide models and attempts synthesis using these methods.

Finally chapter 6 concludes all these discussions and also gives the scope for future work in this area.

1.4 Literature Survey

Although acoustics is a very old branch of science which has been studied for several centuries now, the study of these musical pillars is a very recent area of research. The first systematic study of the musical pillars of Vitthala temple at Hampi was done in 2008 [2], which was continued in [3]. These articles were the main reference and motivation for this thesis. However, several other books and articles were used for studying the theory of beam modelling, linear prediction, digital waveguide (DWG) modelling, etc. In this section, some of the major works that helped the study extensively are discussed. A complete list of references is given at the end of the thesis.

1.4.1 Study of Musical Pillars

The work by Dr. Anish Kumar et al [2] was the motivation for this thesis as it is the first published work in this area. The authors did a very systematic study including different non-destructive tests to find out the material of the pillar and its properties. They also did measurement of dimensions of the musical columns, i.e., *diameter* and *length* of columns. The analysis of sounds from pillars was done. Euler-Bernoulli beam model was discussed in brief to find the flexural frequencies of vibration of the columns and were compared with the measured values.

Patil et al continued this work in [3]. Here, they did a comparison of the spectrum of bell-like sound from pillar with that of an actual bell-like sound. The frequencies were found to be in close agreement. They also did the Euler-Bernoulli modelling of columns of the pillar producing bell sound and obtained the envelopes of the first four mode-shapes of the columns. From a signal processing perspective, the analysis of pillar sound using Iterative energy separation algorithm for instantaneous frequency estimation was done. For this thesis, only spectrum analysis and beam modelling were referred.

1.4.2 Beam Modelling

The theory of beam modelling is widely used in mechanics. There are mainly four beam models and those are discussed in [10]. The authors have explained the differences between all the models and have compared the performances of each of them under different boundary conditions.

This thesis is concerned with only Euler-Bernoulli and Timoshenko models. A book by S. P. Timoshenko [12] was referred for the detailed derivations of Euler-Bernoulli and Timoshenko models. The landmark papers by S. P. Timoshenko ([11, 13]) on Timoshenko model also helped in understanding Timoshenko model. These papers explains the effect of *rotation* and *shear* on the beams. For the solution of Timoshenko model [15] was referred. It discusses the procedure to solve the complex differential equation of the model. Several other books ([16, 14]) and web sources ([17, 18]) helped in modelling the musical columns.

1.4.3 Linear Prediction

The technique of linear prediction is used mostly in speech processing applications. [20] discusses the theory of linear prediction and concatenated tube model in detail. The paper [19] by B. S. Atal and S. L. Hanauer also explains the application of linear prediction in speech processing domain. For details regarding Levinson recursion, [21] was referred.

1.4.4 Digital Waveguide Modelling

Modelling musical instruments as waveguides was studied in detail by J. O. Smith in [25]. This paper describes only one-dimensional waveguides. The ideal waveguide model is discussed first and then different losses are incorporated. The online book by J. O. Smith [23] also helped to get an introduction into the field. The study for two and three dimensional waveguide models were aided by [26] and [27].

1.5 Contributions of this thesis

A study of the published works in this area helped in identifying the limitations of those works. A part of this thesis is an extension of earlier work. However, some concepts from other areas of research like musical instrument modelling and speech processing are also introduced to this problem domain. The major contributions of this thesis are listed below.

- Use of Timoshenko theory to model the vibrations of musical columns.
- Use of digital waveguide model to synthesize sound from pillars.
- Introduction of linear prediction analysis for musical columns.

1.6 Chapter Summary

In this chapter, the Vitthala temple and its musical pillars were introduced. The problem under study and the main parts of it were described. The organization of the thesis into different chapters was also discussed.

In the next chapter, a detailed dimensional analysis of the musical pillars, the techniques used for it and some values of dimensions are given. In addition, the characteristics of the sound produced from the pillars are studied in an attempt to compare them with sound of actual musical instruments.

CHAPTER 2
Dimensional and Spectral Analysis of Pillars and the Sounds Produced

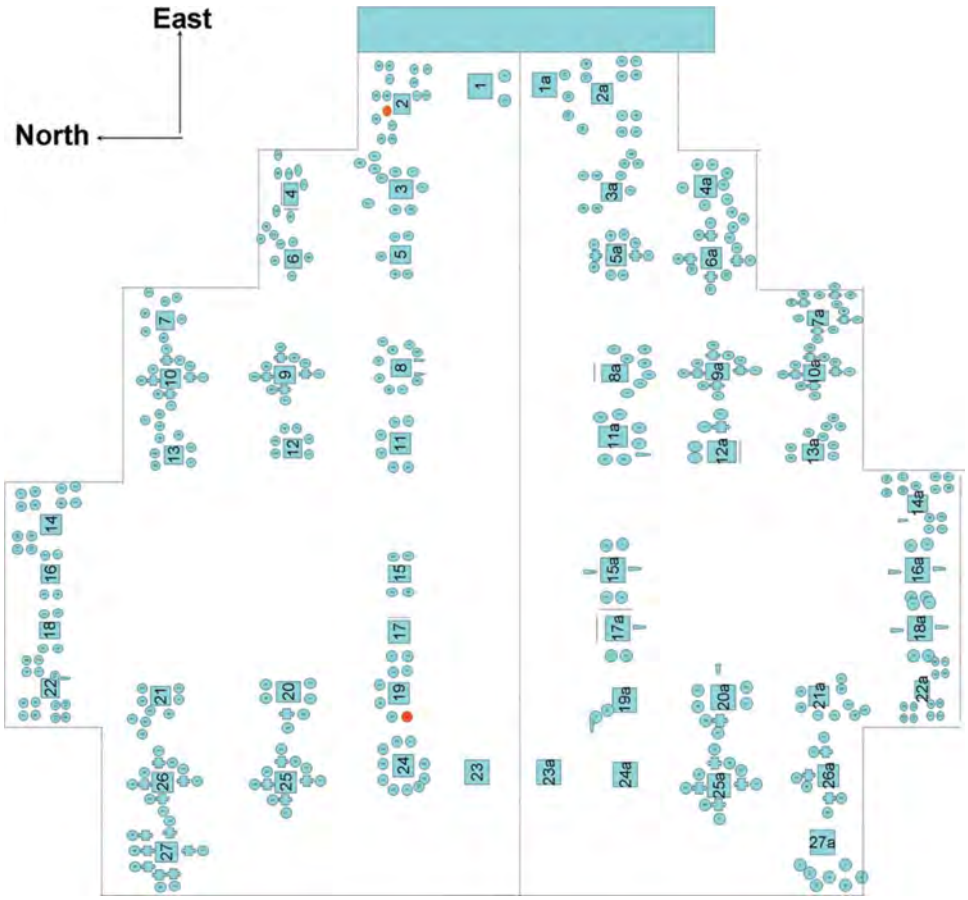
2.1 Introduction

In this chapter, the properties and dimensions of the pillars under study are examined. This data plays a vital role in the study. The dimensions of the musical columns are essential for their theoretical study involving beam modelling and various other synthesis methods.

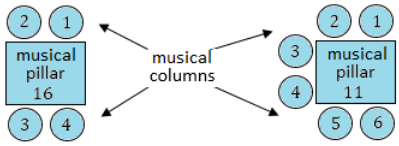
Further, this chapter looks into the characteristics of the sound produced from various pillars. The sound data recorded from one of the *11* pillars are plotted and the spectral characteristics are analysed.

2.2 Dimensional Measurements

The *56* pillars of the Mahamandapam of the temple are arranged as shown in figure 2.1a. Figure 2.1b also shows pillars *11* and *16* in detail. These pillars produce the sound of bell and veena respectively and are used for analysis throughout this thesis. The numbering of the pillars is as reported in [2]. *40* of them are arranged so that it forms an aisle and the other *16* are arranged in a rectangular shape in the middle. The number of columns in a pillar ranges from *4* to *15* [2]. All the columns of some of the pillars are damaged. Each pillar is around *3.6 m* high and measures around *1.5 m* across. The pillars as well as the other structures in the temple are made of granite stone. The musical columns of the pillars have varying diameter [2]. It is maximum at the bottom and decreases gradually as it goes up. However, the maximum variation in diameter is only *10* % across a length of *1 m* of the column. Hence, the columns can be considered cylindrical for practical purposes, taking the average diameter. A detailed dimensional measurement was done by the authors in [2] which is given in the next section.



(a)



(b)

Figure 2.1: Arrangement of pillars in the Mahamandapam. Adapted from [2].

2.3 Non-Destructive Testing

Non-destructive testing (NDT) techniques are methods to study the properties of a material or a system without damaging it [5]. These are very popular methods in research, because they do not cause any permanent alteration to the system being inspected. NDT methods generally rely upon electromagnetic radiations,sound waves or other penetrating radiations to examine the internals of a system [5]. The main applications of NDT methods are in the area of weld verification, structural mechanics, radiography in medicine, etc.

Non-destructive testing techniques were the best choice to study the pillars since it ensures the safety of the musical pillars. Different methods done on the

pillars were low frequency ultrasonic testing, impact echo testing and In-situ metallography. Low frequency ultrasonic testing helps to assess the internal structure of the pillar. A pair of ultrasonic transducers were used for this purpose, one in *transmission* mode and the other in *receiver* mode. The transmitter transducer is coupled to the musical columns using grease as couplant and generates sound waves. The receiver transducer placed on the diametrically opposite side catches the arrival of the waves and the time of travel of the ultrasonic waves is calculated [2]. Impact echo testing measures the impact wave velocity in the columns. It involves introducing a transient stress pulse into the test object by mechanical impact and monitoring the surface displacements caused by the arrival of reflections of the pulse from internal defects and external boundaries. In situ metallography studies are carried out to identify the material of the columns and to study the presence of microcracks [2]. The results of the dimensional measurements and the non-destructive testing methods are given at the end of this chapter in table 2.3.

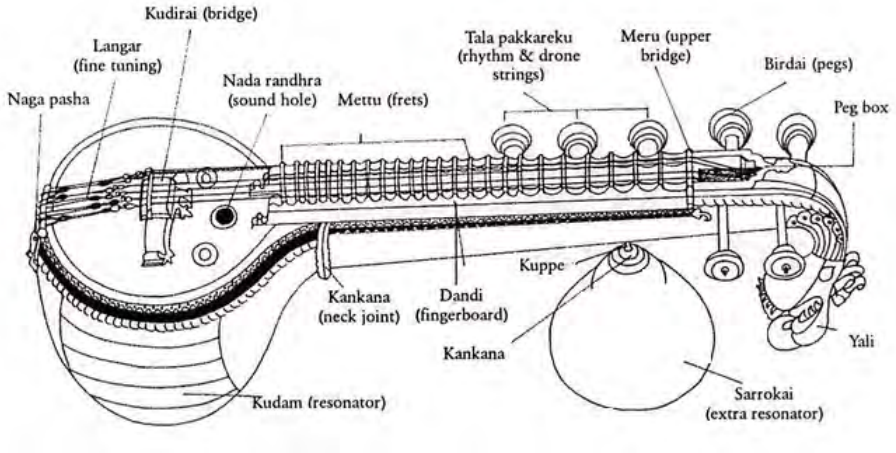
2.4 The Veena Pillar

For calculating the values of fundamental frequency of vibration of each columns, or for synthesizing the sound from musical columns, the dimensions of those columns should be known. For the current study, data for the pillar producing sound of Veena is used. Veena is a string instrument which is widely used in Indian classical music. There exists several variations of Veena. While Saraswati Veena is more popular in the south indian (Carnatic) classical music, Rudra Veena or Vichitra Veena is more used in north indian (Hindustani) classical music. Figure 2.2 shows an image of a Saraswati Veena and its various parts.

In the mahamandapam of Vitthala temple, there is a pillar which produces the sound of Veena. It is shown in figure 2.1a numbered as *16*. The pillar has four musical columns in it. The pictures of this pillar from different angles is shown in figure 2.3, showing its different columns. The maximum and minimum diameter of these columns, their lengths, ultrasonic wave velocity through them and the frequency of sound produced where measured by the authors of [2]. Details are given in table 2.1.



(a) Saraswati Veena. Adapted from [6].



(b) Parts of a Veena. Adapted from [7].

Figure 2.2: A Saraswati Veena and its parts.

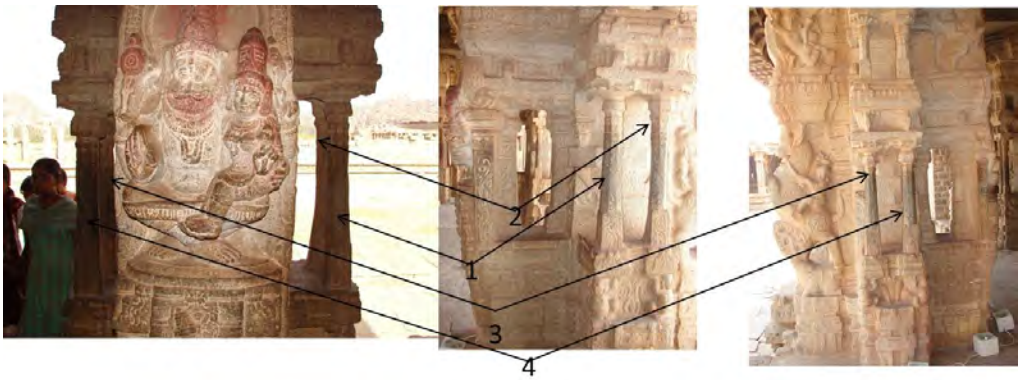


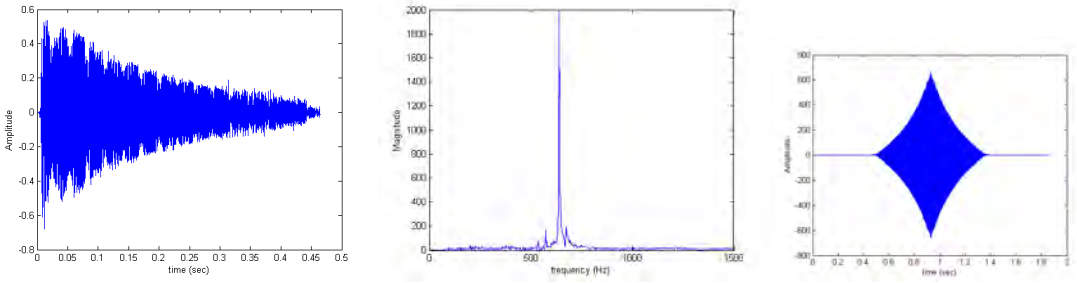
Figure 2.3: Three different views of the Veena pillar. (Photo provided by the lead author of [2]).

Table 2.1: Dimensions of the Veena pillar, provided by the lead author of [2].

Column number	Height (m)	Diameter (mm)		Velocity (m/s)	No. of faces	Frequency (Hz)
		Min	Max			
1	0.84	95.49	113	5300	8	745
2	0.83	101.86	111.41	5250	8	880
3	0.975	92.31	108.23	5300	8	811
4	0.98	98.68	105.04	5100	8	821

2.5 Analysis of Sound from Musical Pillars

The sound produced by striking at the middle of the musical columns with the thumb were recorded. If the object used to give excitation is changed, the amount of contact, the pressure with which it is struck etc. will change. This may lead to changes in output. During data collection by Anish Kumar et al, care was taken that the same person strikes the columns with the same thumb so that the variability in excitation is reduced to some extent. Typical plots of time-domain, frequency-domain and autocorrelation of such sounds are given in figure 2.4.



(a) Plot of time-domain signal (b) Corresponding spectrum (c) Autocorrelation

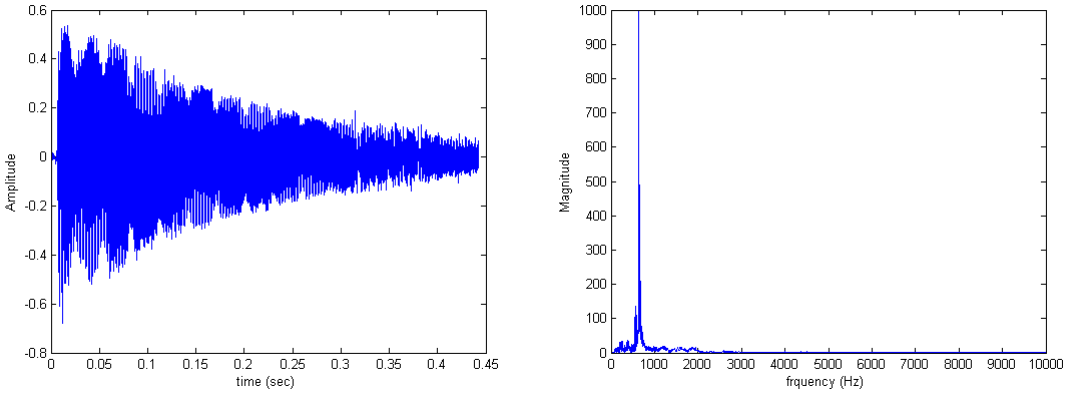
Figure 2.4: Typical plots for sound from pillar. (Sound provided by Prof. Sharada Srinivasan).

Here, half the width of the autocorrelation function at $1/20^{th}$ of the peak amplitude is considered as a parameter related to the decay rate of the sound produced [2]. A higher value of this indicates lower attenuation rate and vice-versa. The width of the time-domain signal at that point is not used so as to avoid error arising due to the noise during recording. This decay time and average duration of sounds from various pillars are also given in [2]. From those data, it is observed that the pillars which are damaged produce sounds of very less duration as compared to the other pillars. The sound from the pillar which is known to produce

bell-like sound exhibited maximum duration [2]. It also has an exponential decay of the sound sample, inharmonic components and nearby peaks in the amplitude spectrum which are the characteristic features of *bell-like* sounds [9]. It is also interesting to note that the time domain signal of the sound from the pillar is similar to the impulse response of an LTI resonator which is a damped sinusoid. Hence the musical columns also can be considered as LTI resonators. The system may not be time invariant. However, in the case of musical columns, the input is given manually using a thumb. The invariance of input over time also cannot be guaranteed. The same is the case with speech production as well. For practical purposes, we approximate it to be an LTI system.

2.5.1 Spectral Analysis

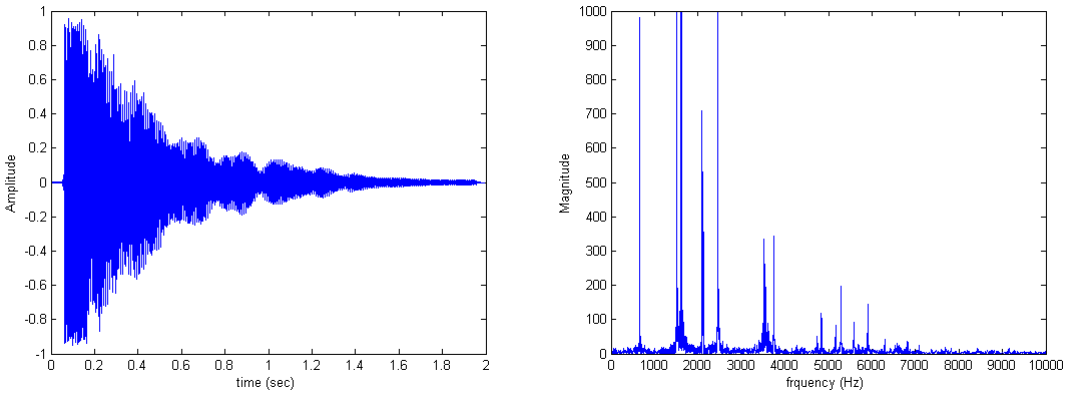
In [3], they have studied the spectral characteristics of the bell-like sound from pillar and compared it with the actual bell sound. The sound from pillar was recorded by striking the columns of the pillar with the thumb. The time and frequency domain plots of the sound from pillar and the actual sound are given in figures 2.5 and 2.6 respectively.



(a) Time-domain signal (b) corresponding spectrum

Figure 2.5: Plot of bell-like sound from pillar.

Analysing the spectra of both the sounds, it can be seen that the 1^{st} peak in both the cases occur at nearby frequencies. However, the sound from the pillar shows only one dominant peak whereas the actual bell sound shows a number of spectral peaks. One of the reasons for this might be the poor quality of sound recorded from the pillar. Since a systematically recorded sound was not available for analysis, sound recorded under noisy conditions was used. In addition, the recorded sound from the pillar is of very short duration, after which the sound is



(a) Time-domain plot (b) corresponding spectrum

Figure 2.6: Plot of actual temple bell sound, sound source: [29].

cut. The exact values of the frequencies corresponding to the peak are shown in table 2.2 for both the sounds.

Table 2.2: Frequencies of actual and pillar sound.

sound	f_1 (Hz)
Actual sound	658.7
Pillar sound	638.1

From table 2.2, it is observed that the frequency of the sound from pillar differs from the frequency of actual sound by only *3.1* %.

Table 2.3: Dimensions of *11* pillars in detail. Adapted from [2].

Pillar number	Corresponding musical instrument	No.of columns in the pillar	Total height range (mm)	Diameter range (mm)	Ultrasonic velocity range (m/s)	Frequency range of sound produced (Hz)	
						Lower	Higher
2 (east)	Saptaswara	8	960 – 1180	75.6 – 99.5	5300 – 5500	243 – 396	687 – 1000
2 (north)	...	6 + 1 (cut)	960 – 1140	89 – 104	5250 – 5430	296 – 372	738 – 967
3	Panchtala	9	870 – 950	62.5 – 100.5	4600 – 5300	442 – 588	1046 – 1280
4	Jaltarang	7	880 – 920	90.0 – 130	5400 – 5500	495 – 780	-
5	Mridanga	5	910 – 985	98 – 106.5	5300 – 5500	444 – 457	1148
11	Ghanta	6	910 – 985	102.7 – 111.2	5400 – 5740	533 – 656	953
14	Ghatam	12	1220 – 1250	102.7 – 122.5	5300 – 5600	305 – 454	774
16	Veena	4	830 – 980	100.3 – 106.6	5200 – 5500	745 – 821	-
24	Tabla	10	1115 – 1120	97.3 – 107.0	5200 – 5600	296 – 497	-
3*A*	Damaru	9	1170 – 1220	97.1 – 106.6	5200 – 5700	273 – 375	739 – 786
5*A*	Kerala Mridangam	5	1080 – 1130	115 – 122	5500 – 5600	338 – 412	783 – 901
20*A*	Sankha	5	940 – 1065	95.5 – 1127.5	5200 – 5450	399 – 471	983 – 1060
15*A*	Damaged	-	-	-	4200	680 – 760	-

2.6 Chapter Summary

In this chapter, the dimensional and spectral analysis of musical pillars were done. The dimensions of the columns of different pillars were shown with an emphasis to the pillar producing sound of Veena. Exact dimensions were available only for that pillar. In addition, the characteristics of typical sounds from the pillars were studied. A comparison of actual and pillar sounds were done for the pillar producing bell-like sound.

In the next chapter, two different beam modelling techniques are discussed in detail. Using these models on the pillars, the flexural frequency of vibration of the musical columns are found. These values are then compared with the measured frequencies.

CHAPTER 3
Vibration Analysis of Musical Columns using Beam Modelling

3.1 Introduction

A beam is a structural element which resists load by primarily by bending. Generally, for a beam the length is more than the width and thickness. The musical columns of the pillars can also be considered as beam-like structures. Striking by a finger induces transverse vibrations in them. Transverse vibrations in a beam can be analysed and the *flexural* frequencies can be found by different methods. The term *flexure* indicates the bending of a body. The frequency of this bending vibrations is termed as flexural frequency. There are different beam modelling theories in the literature which models the vibration. This chapter discusses two major beam modelling techniques which are the Euler Bernoulli/classical beam theory and the Timoshenko beam theory. The flexural frequencies are calculated using both the theories and the correlation with the measured sound frequency from the pillar is investigated. It is to be noted that the measured frequency itself might have errors. However, in the case of musical pillars, there is no ground truth available regarding the frequency of vibration. Hence in all analyses, the measured frequency is considered as the ground truth with which the results are compared.

3.2 Modelling a Transversely Vibrating Beam

It was observed earlier by researchers that the most important factor in a transversely vibrating beam is the *bending* effect. The Euler-Bernoulli beam considers only the kinetic energy due to lateral displacement and the strain due to bending [10]. It is the simplest and most commonly used beam theory also called as the classical beam theory . For many natural cases of beam bending, Euler-Bernoulli

beam provides reasonable approximation. However, the natural frequencies of higher modes are slightly overestimated by this theory. The model works better for *slender* beams (having very less width in proportion to height) than *non-slender* beams [10]. Slight improvements to Euler-Bernoulli theory was provided by the Rayleigh and Shear beam models [10]. Rayleigh model adds the effect of *rotary inertia* also to Euler-Bernoulli model whereas the shear model adds *shear* effect. It was S. P. Timoshenko who proposed an improved beam theory which adds the effects of both rotation and shear to the classical beam theory. This is a major improvement particularly in the case of non-slender beams and for high frequency responses since shear and rotary effects are not negligible in those cases [10].

There are some assumptions made by all the beam theories in common [10]. Some of them are as follows.

- Uniform density throughout the length of the beam.
- Axial dimension is considerably larger than the other two. If the columns are considered in a three dimensional space, the axial dimension is along the length of the column and the dimensions which are perpendicular to the axis are taken as width and thickness.
- Cross-sectional area is symmetric.
- Material is linear elastic.
- Planes perpendicular to the neutral axis remain perpendicular after deformation. Neutral axis is the axis which passes along the beam length where there is no longitudinal stress or strain. For symmetric structures, it coincides with the centroidal axis. The points on one side of this axis undergoes compression and the points on the other side undergoes tension/expansion.
- Angle of rotation is so small that the small angle assumption holds good. The small angle assumption says that the angle is small enough to approximate $\sin\theta \approx \theta$ and $\tan\theta \approx \theta$.

3.3 Beam Equilibrium Equations

Consider a beam undergoing transverse vibration. For ease of analysis, the motion of different parts of the beam can be analysed separately. The whole structure is divided into smaller beam elements which behaves in similar manner under excitation. An example for such a beam element is given in figure 3.1b. For such a

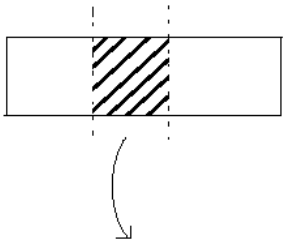
beam element, the net force and moment acting on it must be zero for it to be in equilibrium. If the upward forces and anticlockwise moments are taken as positive, the vertical force and moment equilibrium equations are as follows [16].

$$\frac{\Delta V}{\Delta x} = -w, \tag{3.1}$$

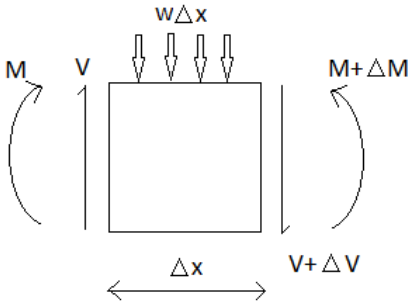
$$\frac{\Delta M}{\Delta x} = V - w\frac{\Delta x}{2}, \tag{3.2}$$

where V is the shear force, M is the moment and w is the applied force. As the width of the beam element tends to zero, equations (3.1) and (3.2) become differential equations which can be combined.

$$\begin{aligned} \frac{dV}{dx} &= -w, \\ \frac{dM}{dx} &= V, \\ \frac{\partial^2 M}{\partial x^2} &= -w. \end{aligned} \tag{3.3}$$



(a) A complete beam



(b)

Figure 3.1: Elementwise analysis of beams.

3.3.1 The Elastic Flexure Formula

Consider the beam given in figure 3.2.

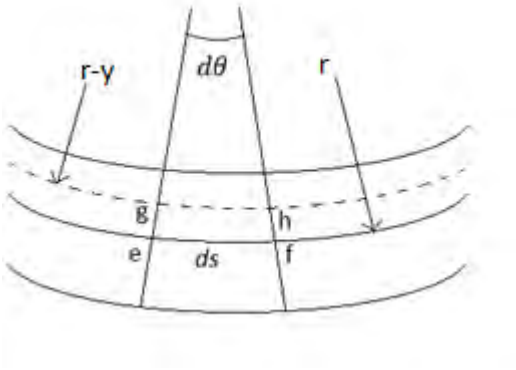


Figure 3.2: A beam undergoing bending.

The arc length ef is [16],

$$\begin{aligned} ds &= rd\theta, \\ \Rightarrow \frac{d\theta}{ds} &= \frac{1}{r} = \kappa, \end{aligned} \tag{3.4}$$

where ds is the arc length, $d\theta$ is the angle formed by the sides of the beam element due to bending and r is the radius of curvature of the neutral axis. The change in length of arc gh due to bending can be written as follows.

$$gh - ef = (r - y)d\theta - rd\theta = -yd\theta. \tag{3.5}$$

Using equations (3.4) and (3.5), the *strain* and *stress* in the element can be found, i.e.,

$$\frac{gh - ef}{ef} = \epsilon = -\kappa y, \tag{3.6}$$

$$\sigma = -\epsilon\kappa y. \tag{3.7}$$

The force corresponding to this stress will cause a moment about the neutral axis of the beam. The moment caused by all such elements are taken [16].

$$M = \int_{bottom}^{top} y\delta F = -E\kappa \int_{bottom}^{top} y^2 \delta A = E\kappa I, \tag{3.8}$$

where E is the elastic modulus of the material of the beam, F is the force caused by one element A is the area of cross-section and I is the area moment of inertia.

Therefore,

$$\kappa = -\frac{M}{EI}. \tag{3.9}$$

If the angle of rotation is negligibly small, then $\theta \approx \tan\theta = \frac{dy}{dx}$ and $ds \approx dx$. Substituting this in equation (3.4) and then using equation (3.9), the elastic flexure formula is obtained as given below [16].

$$-EI\frac{\partial^2 y}{dx^2} = -M. \tag{3.10}$$

3.4 Euler-Bernoulli Model for Musical Columns

The dimensions of the musical columns are such that the height of the column is much larger than the diameter. Hence, they can be considered as slender beams [15]. The lateral loads at both ends of the columns are much larger so that the shear and rotary deformations are small. Therefore, the classical beam theory can be used in this case [3]. For simplicity, the columns are considered as cylindrical with diameter equal to the average of the minimum and maximum diameters [2]. Differentiating the flexure equation (equation (3.10)) twice, and assuming that the vibrating bar is loaded with inertia forces which is opposite to the applied force, the equation of motion for bending modes of homogeneous columns with uniform cross-section is obtained ([8], [2], [3]).

$$EI\frac{\partial^4 y}{\partial x^4} + \rho A\frac{\partial^2 y}{\partial t^2} = 0, \tag{3.11}$$

where ρ is the mass density, κ is the radius of gyration ($D/4$ for cylindrical bars), D is the diameter and $y(x)$ is the deviation from the rest position. In addition, radius of gyration $\kappa = \sqrt{I/A}$.

3.4.1 Solution of Euler-Bernoulli Equation

Assuming that the Euler-Bernoulli equation (equation (3.11)) may be solved by separation of variables [3], the equation for displacement can be written as

$$y(x,t) = \Psi(x)e^{j\omega t}, \tag{3.12}$$

where sinusoidal variation is assumed in time. Therefore,

$$\frac{\partial^2 y}{\partial t^2} = -\omega^2 \Psi(x) e^{j\omega t}, \tag{3.13}$$

$$\frac{\partial^4 y}{\partial x^4} = e^{j\omega t} \frac{d^4 \Psi}{dx^4}. \tag{3.14}$$

Substituting equations (3.13) and (3.14) in the wave equation (equation (3.11)),

$$\frac{d^4 \Psi}{dx^4} = \frac{\omega^2 \rho}{E\kappa^2} \Psi(x) = \frac{\omega^2}{c^2 \kappa^2} \Psi(x) = \frac{\omega^4}{v^4} \Psi(x), \tag{3.15}$$

where the substitutions $c^2 = E/\rho$ and $v^2 = \omega c \kappa$ are used [3]. To solve this, it is assumed that $\Psi = Ae^{\gamma x}$. Substituting this in equation (3.15),

$$\gamma^4 = \frac{\omega^4}{v^4},$$

$$\gamma^2 = \pm \frac{\omega^2}{v^2},$$

which gives,

$$\gamma = \pm k, \qquad \gamma = \pm jk. \tag{3.16}$$

Note that $k = \omega/v$ is the *wave number*. The complete solution for $y(x,t)$ is a sum of four terms [3], i.e.,

$$y(x,t) = e^{j\omega t}(C_1 e^{kx} + C_2 e^{-kx} + C_3 e^{jkx} + C_4 e^{-jkx}). \tag{3.17}$$

Using the identities $e^{\pm x} = \cosh x \pm \sinh x$ and $e^{\pm jx} = \cos x \pm j \sin x$, this can also be written as follows.

$$y(x,t) = e^{j\omega t}[C_1 \cosh(kx) + C_2 \sinh(kx) + C_3 \cos(kx) + C_4 \sin(kx)]. \tag{3.18}$$

or equivalently,

$$\begin{aligned} \Psi(x) = {} & C_1(\cos(kx) + \cosh(kx)) + C_2(\cos(kx) - \cosh(kx)) + \\ & C_3(\sin(kx) + \sinh(kx)) + C_4(\sin(kx) - \sinh(kx)). \end{aligned} \tag{3.19}$$

Note that the constants in equation (3.19), equation (3.18) and equation (3.17) are different. Applying this solution in Euler-Bernoulli wave equation, i.e., equation

(3.11) implies,

$$\begin{aligned} -\omega^2 \Psi(x) e^{j\omega t} &= -\frac{E\kappa^2}{\rho} k^4 \Psi(x) e^{j\omega t}, \\ \omega^2 &= \frac{E\kappa^2}{\rho} k^4. \end{aligned} \tag{3.20}$$

Taking square root of equation (3.20) and dividing by 2π, the frequency can be obtained [2].

$$f = \frac{D}{4} \frac{(kl)^2}{2\pi l^2} \sqrt{\frac{E}{\rho}}, \tag{3.21}$$

where l is the length of the beam.

3.4.2 Boundary Conditions

Differential equations are *point* properties of systems. The solution of a partial differential equation (PDE) will be different for different boundary conditions. The musical columns under consideration are *clamped* at both ends to the pillar as shown in figure 3.3.

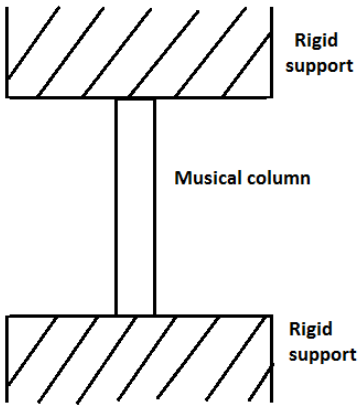


Figure 3.3: Musical column clamped at both ends.

Therefore, the displacement and its derivative are *zero* at both the ends. This forms the boundary conditions for finding the coefficients in the complete solution [3].

$$y = 0, \frac{\partial y}{\partial x} = 0 \qquad \text{at} \qquad x = 0, x = l. \tag{3.22}$$

Applying these boundary conditions in equation (3.19) at $x = 0$ leads to

$$C_1 = C_3 = 0, \tag{3.23}$$

and hence, the boundary conditions at $x = l$ leads to

$$C_2(\cos(kl) - \cosh(kl)) + C_4(\sin(kl) - \sinh(kl)) = 0, \quad (3.24)$$

$$-C_2(\sin(kl) - \sinh(kl)) + C_4(\cos(kl) - \cosh(kl)) = 0. \quad (3.25)$$

This is a system of two homogeneous equations with two unknowns. Since the solution $y(x,t)$ cannot be completely zero, equations (3.24) and (3.25) should have a *non-trivial* solution [3]. Hence, the determinant of coefficients is set to zero, i.e.,

$$\begin{vmatrix} \cos(kl) - \cosh(kl) & \sin(kl) - \sinh(kl) \\ \sin(kl) - \sinh(kl) & \cos(kl) - \cosh(kl) \end{vmatrix} = 0. \quad (3.26)$$

Solving this, the *frequency equation* is obtained as

$$cos(kl)cosh(kl) = 1. \quad (3.27)$$

If $k_n l$ is the n^{th} root of the frequency equation (equation (3.21)), then

$$f_n = \frac{D}{4}\frac{(k_n l)^2}{2\pi l^2}\sqrt{\frac{E}{\rho}}. \quad (3.28)$$

The numerical values of $k_n l$ can be calculated by Newton-Raphson method [3]. The first four roots for the first four modes are given in table 3.1. The eigen modes of the beam corresponding to these four modes are shown in figure 3.4.

Table 3.1: First four roots of the frequency equation.

Mode(n)	1	2	3	4
$k_n l$	4.73	7.8532	10.9956	14.1312

The fundamental frequency of vibration of the columns can be calculated using the first root in table 3.1.

$$f_1 = \frac{(4.73)^2}{8\pi}\frac{D}{l^2}\sqrt{\frac{E}{\rho}} = 0.89\frac{D}{l^2}\sqrt{\frac{E}{\rho}}. \quad (3.29)$$

By substituting the values of properties of the material and dimensions of a musical column, the fundamental frequency of vibration of that particular column can be calculated.

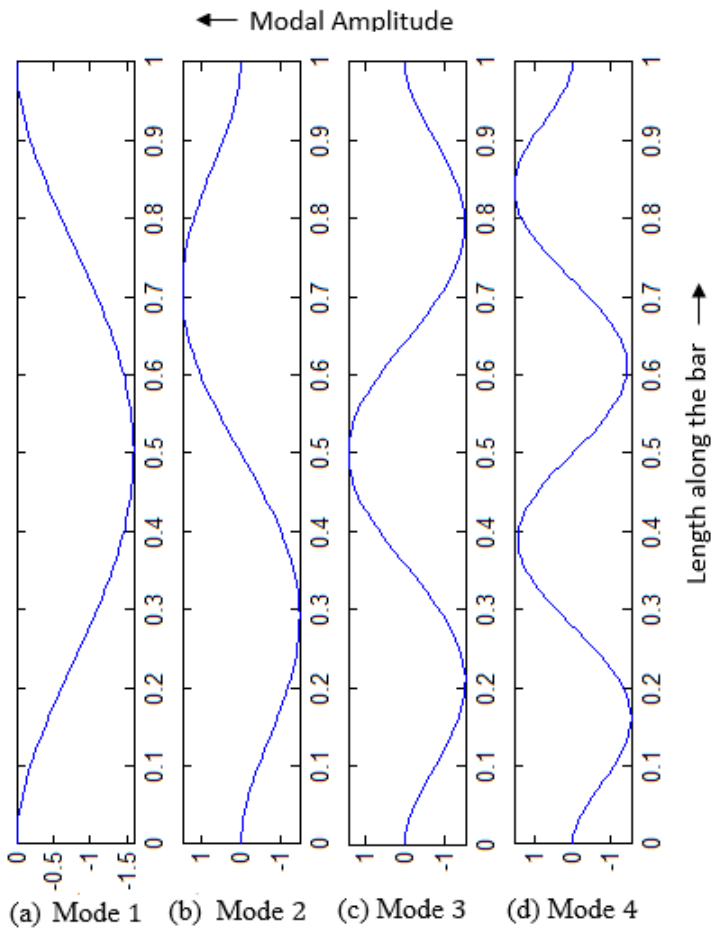


Figure 3.4: The first four mode-shapes of the beam using Euler-Bernoulli model

3.5 Timoshenko Beam Model for Musical Columns

As discussed earlier in section 3.2, the Timoshenko model incorporates the effect of rotation and shear into the Euler-Bernoulli model's equation. During vibration, the elements of the bar undergo not only translation but also rotation [12]. The angle of rotation is equal to the slope of the deflection curve. The corresponding angular acceleration will be given by,

$$\frac{\partial^2 \theta}{\partial t^2} = \frac{\partial^3 y}{\partial^2 t \partial x}. \tag{3.30}$$

Thus, the moment of inertia forces due to this rotation about the axis for a single beam element should as well be incorporated in the moment equilibrium equation, i.e., equation(3.3).

$$\frac{dM}{dx} = V - I\rho \frac{\partial^3 y}{\partial^2 t \partial x}. \tag{3.31}$$

Hence, the deflection equation including the effect of rotation is [11]

$$EI\frac{\partial^4 y}{\partial x^4} = -\rho A\frac{\partial^2 y}{\partial t^2} + I\rho\frac{\partial^4 y}{\partial x^2 \partial t^2}. \tag{3.32}$$

A more accurate deflection equation can be obtained if the deflection due to shear is also taken into consideration. The total slope of the deflection curve will now have the shear component as well [11]. If ψ is the slope without considering shear and β is the shear angle, then the slope is,

$$\frac{dy}{dx} = \psi + \beta. \tag{3.33}$$

The elementary beam theory [12] says,

$$M = -EI\frac{d\psi}{dx}, \tag{3.34}$$

$$V = k'\beta AG = k'\left(\frac{dy}{dx} - \psi\right)AG. \tag{3.35}$$

Here, k' is called the *shear correction* factor. The moment equilibrium equation and vertical force equilibrium equation now becomes,

$$\rho A\frac{\partial^2 y}{\partial t^2} - k'GA\left(\frac{\partial^2 y}{\partial x^2} - \frac{\partial \psi}{\partial x}\right) = 0. \tag{3.36}$$

$$EI\frac{\partial^2 \psi}{\partial x^2} + k'GA\left(\frac{\partial y}{\partial x} - \psi\right) - I\rho\frac{\partial^2 \psi}{\partial t^2} = 0. \tag{3.37}$$

Equations (3.36) and (3.37) form the coupled differential equations of Timoshenko beam theory [11].

3.5.1 Solution of Timoshenko Beam Equation

Both y and ψ are functions of position (x) as well as time (t). However, separation of variables is assumed for solving the equation [15].

$$y(x,t) = X(x)T(t), \quad \psi(x,t) = Y(x)T(t) \tag{3.38}$$

Using these substitutions in the coupled equations for Timoshenko beam (Equations (3.36) and (3.37)),

$$\rho AX(x)\ddot{T}(t) - k'GA\left(T(t)X''(x) - T(t)Y'(x)\right) = 0, \tag{3.39}$$

$$EIT(t)Y''(x) + k'GA\left(T(t)X'(x) - Y(x)T(t)\right) - I\rho Y(x)\ddot{T}(t) = 0, \tag{3.40}$$

where $\dot{T} = \frac{dT}{dt}$, $X' = \frac{dX}{dx}$ and $Y' = \frac{dY}{dx}$. As in the case of Euler-Bernoulli model, it is assumed that the motion in time is sinusoidal, i.e.,

$$T(t) = e^{j\omega t} \;\Rightarrow\; \ddot{T}(t) = -\omega^2 T(t).$$

Thus, equations (3.39) and (3.40) becomes,

$$\begin{aligned} \rho A\omega^2 X(x) - k'GA\left(X''(x) - Y'(x)\right) = 0, \\ EIY''(x) + k'GA\left(X'(x) - Y(x)\right) + I\rho\omega^2 Y(x) = 0, \end{aligned}$$

which can be written as,

$$X''(x) + aX(x) - Y'(x) = 0, \tag{3.41}$$

$$Y''(x) + bY(x) + cX'(x) = 0. \tag{3.42}$$

where $a = \omega^2\rho/k'G$, $c = k'GA/EI$ and $b = (\omega^2\rho/E) - c$ [15]. From the above equations (3.41) and (3.42),

$$\begin{aligned} Y(x) &= -\frac{1}{b}\left[Y''(x) + cX'(x)\right], \\ Y'(x) &= X''(x) + aX'(x), \\ \Rightarrow Y''(x) &= X'''(x) + aX'(x). \end{aligned}$$

Hence, the decoupled differential equation in y for the Timoshenko beam theory [11, 15] is obtained.

$$X^4(x) + (a+b+c)X''(x) + abX(x) = 0,$$

or taking $d = a + b + c$ and $e = ab$,

$$X^4(x) + dX''(x) + eX(x) = 0. \tag{3.43}$$

Giving d and e its values,

$$\frac{d^4}{dx^4}X(x) + \frac{\rho\omega^2}{E}\left(1 + \frac{E}{k'G}\right)\frac{d^2}{dx^2}X(x) + \frac{\omega^2}{EI}\left(\omega^2\rho^2\frac{I}{k'G} - \rho A\right)X(x) = 0. \tag{3.44}$$

To solve this equation, the characteristic equation corresponding to this differential equation is found as follows [14].

$$D^4 + dD^2 + e = 0. \tag{3.45}$$

Substituting $D^2 = r$, it becomes

$$r^2 + dr + e = 0. \tag{3.46}$$

The roots of this equation are,

$$r_1 = \frac{-d + \sqrt{\Delta}}{2}, \tag{3.47}$$

$$r_2 = \frac{-d - \sqrt{\Delta}}{2}, \tag{3.48}$$

where $\Delta = d^2 - 4e = \omega^4\rho^2 I^2 \left(1 - \frac{E}{k'G}\right)^2 + 4EI\omega^2\rho A$. It can be observed that $\Delta, d > 0 \ \forall \ \omega$ (E, I, k', G, ρ, A are positive constants) [15]. Therefore,

$$\begin{aligned} r_2 &< 0 \quad \forall\omega, \\ r_1 &> 0 \Rightarrow d < \sqrt{\Delta} \Rightarrow \omega < \sqrt{\frac{Gk'A}{\rho I}}, \\ r_1 &< 0 \Rightarrow \omega > \sqrt{\frac{Gk'A}{\rho I}}. \end{aligned}$$

This implies that there are two cases of solution [15]. Let $\sqrt{|r_1|} = \lambda_1$ and $\sqrt{|r_2|} = \lambda_2$.

Case 1: $\omega < \sqrt{\frac{Gk'A}{\rho I}}$

In this case, r_1 is positive and r_2 is negative. Hence, the roots of the characteristic equation (equation (3.45)) are,

$$D_1 = +\lambda_1, D_2 = -\lambda_1, D_3 = +j\lambda_2, D_4 = -j\lambda_2, \tag{3.49}$$

and the solution of the differential equation takes the form [15],

$$X(x) = C_1 e^{\lambda_1 x} + C_2 e^{-\lambda_1 x} + C_3 e^{j\lambda_2 x} + C_4 e^{-j\lambda_2 x}, \tag{3.50}$$

which can also be written as,

$$X(x) = A_1 \cosh(\lambda_1 x) + A_2 \sinh(\lambda_1 x) + A_3 \cos(\lambda_2 x) + A_4 \sin(\lambda_2 x). \tag{3.51}$$

Case 2: $\omega > \sqrt{\frac{Gk'A}{\rho I}}$

In this case, both r_1 and r_2 are negative. The roots of the characteristic equation (equation (3.45)) in this case are,

$$D_1 = +j\lambda_1, D_2 = -j\lambda_1, D_3 = +j\lambda_2, D_4 = -j\lambda_2. \tag{3.52}$$

Hence, the solution of the differential equation takes the form [15],

$$X(x) = C_1 e^{j\lambda_1 x} + C_2 e^{-j\lambda_1 x} + C_3 e^{j\lambda_2 x} + C_4 e^{-j\lambda_2 x}, \tag{3.53}$$

which can also be written as,

$$X(x) = B_1 \cos(\lambda_1 x) + B_2 \sin(\lambda_1 x) + B_3 \cos(\lambda_2 x) + B_4 \sin(\lambda_2 x). \tag{3.54}$$

3.5.2 Boundary Conditions

As discussed earlier in section 3.4.2, the musical columns are clamped at both the ends. For a clamped end ($x_i = 0$ or $x_i = l$), the boundary conditions are, [15]

- $y(x_i, t) = 0 \Rightarrow X(x_i) = 0$.
- $\psi(x_i, t) = 0 \Rightarrow Y(x_i) = 0 \Rightarrow X'''(x_i) + (a + c)X'(x_i) = 0$.

Now, these boundary conditions are applied in the solutions for both the cases given by equations (3.51) and (3.54).

Case 1:

$$X(x) = A_1 \cosh(\lambda_1 x) + A_2 \sinh(\lambda_1 x) + A_3 \cos(\lambda_2 x) + A_4 \sin(\lambda_2 x),$$

$$X'(x) = A_1\lambda_1 \sinh(\lambda_1 x) + A_2\lambda_1 \cosh(\lambda_1 x) - A_3\lambda_2 \sin(\lambda_2 x) + A_4\lambda_2 \cos(\lambda_2 x),$$

$$X'''(x) = A_1\lambda_1^3 \sinh(\lambda_1 x) + A_2\lambda_1^3 \cosh(\lambda_1 x) + A_3\lambda_2^3 \sin(\lambda_2 x) - A_4\lambda_2^3 \cos(\lambda_2 x),$$

$$\begin{aligned} Y(x) = {} & A_1 \sinh(\lambda_1 x)[\lambda_1^3 + (a + c)\lambda_1] + A_2 \cosh(\lambda_1 x)[\lambda_1^3 + (a + c)\lambda_1] \\ & + A_3 \sin(\lambda_2 x)[\lambda_2^3 - (a + c)\lambda_2] + A_4 \cos(\lambda_2 x)[-\lambda_2^3 + (a + c)\lambda_2]. \end{aligned}$$

$X(0) = 0 \Rightarrow$

$$A_1 + A_3 = 0. \tag{3.55}$$

$Y(0) = 0 \Rightarrow$

$$A_2[\lambda_1^3 + (a+c)\lambda_1] + A_4[-\lambda_2^3 + (a+c)\lambda_2] = 0. \tag{3.56}$$

$X(l) = 0 \Rightarrow$

$$A_1 \cosh(\lambda_1 l) + A_2 \sinh(\lambda_1 l) + A_3 \cos(\lambda_2 l) + A_4 \sin(\lambda_2 l) = 0. \tag{3.57}$$

$Y(l) = 0 \Rightarrow$

$$\begin{aligned} &A_1 \sinh(\lambda_1 l)[\lambda_1^3 + (a+c)\lambda_1] + A_2 \cosh(\lambda_1 l)[\lambda_1^3 + (a+c)\lambda_1] \\ &+A_3 \sin(\lambda_2 l)[\lambda_2^3 - (a+c)\lambda_2] + A_4 \cos(\lambda_2 l)[-\lambda_2^3 + (a+c)\lambda_2] = 0. \end{aligned} \tag{3.58}$$

The above four equations form a matrix equation of the form $Mx = 0$ where M is,

$$\begin{bmatrix} 1 & 0 & 1 & 0 \\ 0 & \lambda_1^3 + (a+c)\lambda_1 & 0 & -\lambda_2^3 + (a+c)\lambda_2 \\ \cosh(\lambda_1 l) & \sinh(\lambda_1 l) & \cos(\lambda_2 l) & \sin(\lambda_2 l) \\ \sinh(\lambda_1 l)(\lambda_1^3 + (a+c)\lambda_1) & \cosh(\lambda_1 l)(\lambda_1^3 + (a+c)\lambda_1) & \sin(\lambda_2 l)(\lambda_2^3 - (a+c)\lambda_2) & \cos(\lambda_2 l)(-\lambda_2^3 + (a+c)\lambda_2) \end{bmatrix}. \tag{3.59}$$

Similar to the case of Euler-Bernoulli solution, this set of equations should have a *non-trivial* solution. For that, it must satisfy

$$det(M) = 0. \tag{3.60}$$

Case 2:

$$X(x) = B_1 \cos(\lambda_1 x) + B_2 \sin(\lambda_1 x) + B_3 \cos(\lambda_2 x) + B_4 \sin(\lambda_2 x),$$

$$X'(x) = -B_1\lambda_1 \sinh(\lambda_1 x) + B_2\lambda_1 \cos(\lambda_1 x) - B_3\lambda_2 \sin(\lambda_2 x) + B_4\lambda_2 \cos(\lambda_2 x),$$

$$X'''(x) = B_1\lambda_1^3 \sin(\lambda_1 x) - B_2\lambda_1^3 \cos(\lambda_1 x) + B_3\lambda_2^3 \sin(\lambda_2 x) - B_4\lambda_2^3 \cos(\lambda_2 x),$$

$$Y(x) = B_1 \sin(\lambda_1 x)[\lambda_1^3 - (a+c)\lambda_1] + B_2 \cos(\lambda_1 x)[-\lambda_1^3 + (a+c)\lambda_1]$$
$$+B_3 \sin(\lambda_2 x)[\lambda_2^3 - (a+c)\lambda_2] + B_4 \cos(\lambda_2 x)[-\lambda_2^3 + (a+c)\lambda_2].$$

$X(0) = 0 \Rightarrow$

$$B_1 + B_3 = 0. \tag{3.61}$$

$Y(0) = 0 \Rightarrow$

$$B_2[-\lambda_1^3 + (a+c)\lambda_1] + B_4[-\lambda_2^3 + (a+c)\lambda_2] = 0. \tag{3.62}$$

$X(l) = 0 \Rightarrow$

$$B_1 \cos(\lambda_1 l) + B_2 \sin(\lambda_1 l) + B_3 \cos(\lambda_2 l) + B_4 \sin(\lambda_2 l) = 0. \tag{3.63}$$

$Y(l) = 0 \Rightarrow$

$$B_1 \sin(\lambda_1 l)[\lambda_1^3 - (a+c)\lambda_1] + B_2 \cos(\lambda_1 l)[-\lambda_1^3 + (a+c)\lambda_1]$$
$$+B_3 \sin(\lambda_2 l)[\lambda_2^3 - (a+c)\lambda_2] + B_4 \cos(\lambda_2 l)[-\lambda_2^3 + (a+c)\lambda_2] = 0. \tag{3.64}$$

The above four equations form a matrix equation of the form $Hx = 0$ where H is,

$$\begin{bmatrix} 1 & 0 & 1 & 0 \\ 0 & -\lambda_1^3 + (a+c)\lambda_1 & 0 & -\lambda_2^3 + (a+c)\lambda_2 \\ \cos(\lambda_1 l) & \sin(\lambda_1 l) & \cos(\lambda_2 l) & \sin(\lambda_2 l) \\ \sin(\lambda_1 l)(\lambda_1^3 - (a+c)\lambda_1) & \cos(\lambda_1 l)(-\lambda_1^3 + (a+c)\lambda_1) & \sin(\lambda_2 l)(\lambda_2^3 - (a+c)\lambda_2) & \cos(\lambda_2 l)(-\lambda_2^3 + (a+c)\lambda_2) \end{bmatrix}. \tag{3.65}$$

This set of equations should have a non-trivial solution. For that,

$$det(H) = 0. \tag{3.66}$$

3.6 Constants in the Solution

Solutions of both Euler-Bernoulli and Timoshenko beam equations have several constants which depends on the material properties and dimensions of the musical column. The material with which the musical pillars are made is *granite*.

The numerical values of these constants for granite stone are as given in table 3.2 [2, 3, 17].

Table 3.2: Properties of granite, Source: [17]

Property	Numerical value
Young's modulus (E)	66 GPa
Shear modulus (G)	26 GPa
Mass density (ρ)	2.6 Mg/m^3
Poisson's ratio (ν)	0.215

The temple was constructed many centuries back [1] and was burned once by invaders [2]. The chances that the properties of the material of construction of the temple have changed over this long period are very high. Therefore, to reduce the dependency of solutions to these many material properties, the solutions can be written in terms of only Poisson's ratio (ν) and the dimensions of the columns. To achieve this, the following substitutions are used [2, 3].

$$\frac{E}{\rho} = V_L \sqrt{\frac{(1+\nu)(1-2\nu)}{(1-\nu)}}, \tag{3.67}$$

$$\frac{E}{G} = 2(\nu+1). \tag{3.68}$$

In addition, I and A can be written in terms of the dimensions of the beam.

$$I = \frac{\pi D^4}{64},$$
$$A = \frac{\pi D^2}{4}.$$

Therefore,

$$\frac{I}{A} = \frac{D^2}{16}. \tag{3.69}$$

Another constant that appears in the solution of Timoshenko beam equation is the shear correction factor (k'). There are several methods to find out the value of shear factor which is dependent on the shape of the cross-section [18]. For most practical purposes, the value can be approximated by an expression in ν. Since the musical columns under consideration are approximated to have uniform circular cross-section, the value of shear correction factor is given by [18] as,

$$k' = \frac{6(1+\nu)}{7+6\nu}. \tag{3.70}$$

Now, the solutions of both the beam theories depend only on the dimensions of the beam which are measured and the Poisson's ratio of the beam material.

3.7 Calculating Flexural Frequency

Using equation (3.67) in equation (3.29), the expression for the fundamental frequency of the musical column using Euler-Bernoulli beam model is obtained as,

$$f_1 = 0.84\frac{DV_L}{l^2}. \tag{3.71}$$

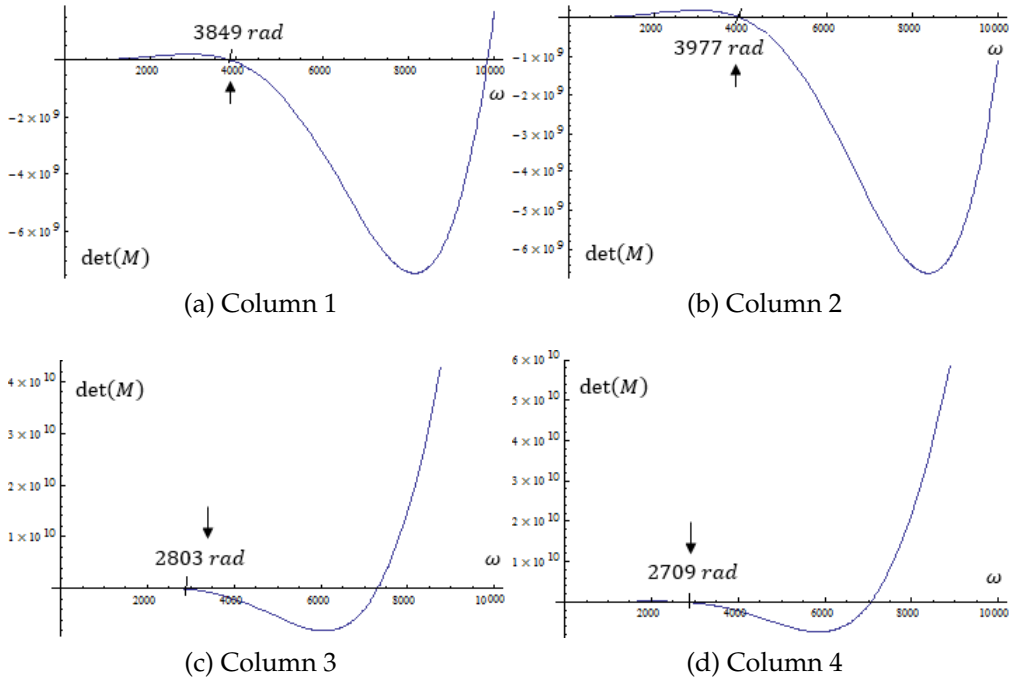
Substituting the values for D, V_L and l for the columns of Veena pillar from table 2.1, the fundamental frequencies for each column can be calculated.

For Timoshenko equation also, equations (3.60) and (3.66) are to be solved after substituting the dimension values. As discussed in section 3.5.1, the Timoshenko beam equation has two cases of solution for two different ranges of ω. The solution changes at the point $\omega = \sqrt{\frac{Gk'A}{\rho I}}$. This value for the columns of Veena pillar is calculated to be of the order of 100 kHz using the properties of granite as given in table 3.2 whereas it can be seen from table 2.1 that for the pillar producing sound of Veena, the measured value of frequency is always less than 1 kHz. Therefore, in our case, only the first case of solution is valid. To solve matrix equations like (3.60), the software *Wolfram Mathematica* was used [28]. The plots of $det(M)$ *vs.* ω for all the four columns of Veena pillar are given in figure 3.5. The exact values of fundamental frequencies were calculated for all 4 columns using both Euler-Bernoulli and Timoshenko beam theories. Table 3.3 shows the results.

Table 3.3: Comparison of frequencies from two beam models

Column	Frequency (Hz)		
	Euler-Bernoulli	Timoshenko	Measured
1	**657.746**	612.552	**745**
2	**682.617**	632.911	**880**
3	469.577	446.073	811
4	454.357	431.203	821

From table 3.3, it can be seen that Euler-Bernoulli beam model gives a closer value of frequency to the measured frequency as compared to the frequency from Timoshenko model for *column* 1 and *column* 2. Although Timoshenko beam model is said to be the best theoretically, a contradicting result is obtained in the case of musical columns. This indicates that the shear and rotation effects are negligibly



(a) Column 1

(b) Column 2

(c) Column 3

(d) Column 4

Figure 3.5: Plots of $det(M)$ *vs* ω for columns of Veena pillar. Arrows indicate the first root of matrix equation corresponding to the fundamental frequency.

small in the case of these musical columns. Another point to note is that, for both the beam theories, the calculated frequency values for *column* 3 and *column* 4 give large deviation from measured values. This can be attributed to the smooth, uniform cross section throughout the length of *column* 1 and *column* 2. For *column* 3 and *column* 4, sharp changes in cross section are observed at top and bottom sides. This can cause formation of nodes at points other than the ends for the 1^{st} mode of vibration, thereby reducing the effective length.

3.8 Chapter Summary

In this chapter, the Euler-Bernoulli and Timoshenko beam models were discussed in detail. Their derivation, solution and finally application onto musical columns were discussed. The flexural frequencies using both the models were calculated and compared with the measured values, for the Veena pillar.

The next chapter describes the concept of linear prediction, which is an important model for analysis and synthesis in speech processing, and its applications on the musical columns.

CHAPTER 4
Linear Prediction (LP) Analysis of Musical Pillars

4.1 Introduction

Linear prediction (LP) is one of the most widely used methods in time series analysis. It has wide applications in many diverse areas like signal processing, economics and geophysics. It is a fundamental tool of analysis in speech signal processing. The most celebrated application of linear prediction in speech literature is in modelling the vocal tract, where it is modelled as an all-pole LTI filter [20]. The musical columns under study are acoustic tubes which produces sound on excitation. Their role in sound production is similar to that of the vocal tract in speech production which gives speech signal as output on excitation. Thus linear prediction which is used in speech analysis can be extended to the musical column analysis also. In this chapter, the possibilities of using linear prediction to model the musical columns are explored.

4.2 Linear Prediction

In natural signals like speech, individual samples will not convey any perceptually significant information. The sequence or neighbourhood information is important as well. For example, the sample at one point could be related with the previous samples in a linear or non-linear way. In *linear* prediction, a signal sample $s(n)$ is assumed to be predictable as a linear combination of previous samples. It can be expressed mathematically in the following way [20].

$$\hat{s}(n) = -\sum_{i=1}^{P} a_i s(n-i), \tag{4.1}$$

where $\hat{s}(n)$ is the predicted signal, $s(n)$ is the actual signal, $a_i's$ are the *linear prediction coefficients* (LPCs) and P is the *prediction order*. The error between the actual and the predicted signal, commonly called as the *LP residual*, has an important role in applications of LP such as speech compression. The LP residual or error signal is denoted as

$$e(n) = s(n) - \hat{s}(n). \tag{4.2}$$

If the coefficients are chosen such that the dependencies are captured correctly, then $\hat{s}(n)$ will be a close estimate of $s(n)$, hence minimising the error [20].

4.3 Finding Optimal LPCs

To minimize the error, the energy (i.e., the l^2 norm) in the LP residual is minimized [20].

$$J = \sum_{n=0}^{N-1} e^2(n). \tag{4.3}$$

Minimising J with respect to the LP coefficients implies that,

$$\frac{\partial J}{\partial a_k} = 0,\ k = 1, 2, ..., P. \tag{4.4}$$

From equation (4.2) and equation (4.3),

$$\begin{aligned} J &= \sum_{n=0}^{N-1} (s(n) - \hat{s}(n))^2, \\ &= \sum_{n=0}^{N-1} [s(n) + \sum_{k=1}^{P} a_k s(n-k)]^2. \end{aligned}$$

Applying this in equation (4.4), and minimising J with respect to the first LP coefficient,

$$\begin{aligned} &\frac{\partial}{\partial a_1} J = 0, \\ &\qquad \Rightarrow \quad \frac{\partial}{\partial a_1} \left\{ \sum_{n=0}^{N-1} [s(n) + \sum_{k=1}^{P} a_k s(n-k)]^2 \right\} = 0, \\ &\qquad \Rightarrow \quad \sum_{n=0}^{N-1} 2 \left(s(n) + \sum_{k=1}^{P} a_k s(n-k) \right) \frac{\partial}{\partial a_1} \left[s(n) + \sum_{k=1}^{P} a_k s(n-k) \right], \end{aligned}$$

$$\Rightarrow \sum_{n=0}^{N-1} s(n)s(n-1) + \sum_{n=0}^{N-1}\sum_{k=1}^{P} a_k s(n-k)s(n-1) = 0,$$

$$\Rightarrow \sum_{k=1}^{P} a_k \left\{ \sum_{n=0}^{N-1} s(n-k)s(n-1) = \right\} = -\sum_{n=0}^{N-1} s(n)s(n-1),$$

$$\sum_{k=1}^{P} a_k R(1-k) = -R(1).$$

Here, the autocorrelation function of the signal $s(n)$ is defined as follows.

$$R(i) = \sum_{n=0}^{N-1} s(n)s(n-i). \tag{4.5}$$

In general, for any LP coefficient a_i, $i = 1, ..., P$,

$$\sum_{k=1}^{P} a_k R(i-k) = -R(i). \tag{4.6}$$

This gives us P equations in P unknowns (a_k, $k = 1, ..., P$) which can be represented in matrix form as [20],

$$\begin{bmatrix} R(0) & R(-1) & \dots & R(1-P) \\ R(1) & R(0) & \dots & R(2-P) \\ \vdots & \vdots & \ddots & \vdots \\ R(P-1) & R(P-2) & \dots & R(0) \end{bmatrix} \begin{bmatrix} a_1 \\ a_2 \\ \vdots \\ a_P \end{bmatrix} = - \begin{bmatrix} R(1) \\ R(2) \\ \vdots \\ R(P) \end{bmatrix}. \tag{4.7}$$

Since autocorrelation is an *even* function, i.e., $R(k) = R(-k)$, equation (4.7) can be rewritten as,

$$\begin{bmatrix} R(0) & R(1) & \dots & R(P-1) \\ R(1) & R(0) & \dots & R(P-2) \\ \vdots & \vdots & \ddots & \vdots \\ R(P-1) & R(P-2) & \dots & R(0) \end{bmatrix} \begin{bmatrix} a_1 \\ a_2 \\ \vdots \\ a_P \end{bmatrix} = - \begin{bmatrix} R(1) \\ R(2) \\ \vdots \\ R(P) \end{bmatrix}. \tag{4.8}$$

It is to be noted that the matrix equation (4.8) contains a *Toeplitz* matrix (A matrix in which elements along any diagonal are the same).

$$T\hat{a}_k = R.$$

The LP coefficient matrix can be found by taking the inverse of the Toeplitz matrix as,

$$\hat{a}_k = T^{-1}R. \tag{4.9}$$

However, finding the inverse of a matrix can be a costly task in real time systems. Therefore, the *Levinson-Durbin* algorithm is used to find the solution of matrix equation (4.8). This algorithm makes use of the Toeplitz property of the matrix to find the solution [21].

4.3.1 The Levinson-Durbin Algorithm

The Levinson-Durbin Algorithm or the Levinson recursion is a recursive algorithm which finds the i^{th} order prediction coefficients from the $(i-1)^{th}$ order coefficients. During each recursion, the mean squared error (MSE) corresponding to that order is minimized to find the optimal solution. Different steps of the Levinson-Durbin algorithm are as follows [20].

Step 1:

Initialize the predictor coefficient of *0* order predictor to zero. Hence, the predicted signal $\hat{s}(n) = 0$. This implies that the mean squared error (MSE) equals the first value of autocorrelation.

$$\begin{aligned} a_0^0 &= 0, \\ E^0 &= r(0). \end{aligned}$$

Step 2:

Find the weighting factor for the i^{th} order predictor, i.e.,

$$k_i = \left(r(i) - \sum_{j=1}^{i-1} a_j^{i-1} r(i-j) \right) / E^{i-1}.$$

Step 3:

Update the coefficients for the i^{th} order predictor using *step 2*.

$$\begin{aligned} a_i^i &= k_i, \\ a_j^i &= a_j^{i-1} - k_i a_{i-j}^{i-1}, \quad 1 \leq j \leq i-1 \end{aligned}$$

The constants k_i are called the *partial correlation coefficients* (also called as *PARCOR* coefficients).

Step 4:

Update the mean squared error for the i^{th} order predictor.

$$E^i = (1 - k_i^2)E^{i-1}.$$

Repeat *step 2* to *step 4* for $i = 1, ..., P$. The P^{th} order coefficients obtained are the desired optimal LP coefficients. The detailed derivation of the Levinson-Durbin algorithm can be found in [21].

4.4 Estimating Prediction Order

In speech processing literature, it has been proved that the order of prediction depends on the length of the vocal tract [19]. The number of coefficients required to represent the speech segment with minimum error is determined by the number of poles and zeros of the vocal tract in the desired frequency range. In order to represent the poles of the vocal tract transfer function, the linear predictor memory must be equal to twice the time required for sound waves to travel across the vocal tract [19]. In the case of musical pillars, the vocal tract length can be replaced by length of the musical column under consideration and the sound velocity in air by the ultrasonic wave velocity through the column. Using the measurements in table 2.1, the number of predictor coefficients needed to find the predicted sound signal from different musical columns of the Veena pillar can be found. For the 1^{st} column with length $l = 0.84 \ \ m$ and ultrasonic wave velocity $v = 5300 \ \ m/s$, the predictor memory should be equal to $2l/v = 0.317\, ms$. Therefore, for a sampling frequency of $48\, kHz$, the number of predictor coefficients required is obtained as 15.22. It can be approximated to the smallest following integer 16.

4.5 The LP Spectrum

According to equation (4.2), the error between actual and predicted signal is,

$$e(n) = s(n) + \sum_{k=1}^{P} a_k s(n-k). \tag{4.10}$$

Taking Z-Transform on both sides,

$$E(z) = S(z)\left[1 + \sum_{k=1}^{P} a_k z^{-k}\right], \tag{4.11}$$

$$\Rightarrow E(z) = S(z)A(z). \tag{4.12}$$

Here, $A(z)$ is an all-zero filter which takes the signal as input and gives a noise-like error / LP residual as output. Ideally, the LP residual has an almost flat spectrum. In speech processing, this implies that the filter $A(z)$ has characteristics similar to the inverse characteristics of the vocal tract. The vocal tract takes the noise like signal from glottis (source in speech production) and gives the speech signal as output [20]. Hence,

$$S(z) = \frac{1}{A(z)}E(z),$$

$$S(z) = H(z)E(z). \tag{4.13}$$

This is the principle behind speech synthesis using linear prediction. Speech signal can be reconstructed from the noise like LP residual if the LP coefficients are known. The spectrum corresponding to the filter $H(z)$ is called the LP spectrum.

The peaks occurring in the LP spectrum may sometimes be blunt. This might make it difficult to locate the frequency value of the peak just by looking at the spectrum. In order to get sharper peaks at those frequency points, the group delay spectrum of $H(z)$ may be considered [22]. Group delay of a signal is defined as the negative derivative of its phase.

$$\tau(\omega) = -\frac{d}{d\omega}\phi(\omega), \tag{4.14}$$

where $\tau(\omega)$ is the group delay in seconds and $\phi(\omega)$ is the Fourier transform phase of the signal. An important property of group delay function is its additive property [22]. The frequency response of a general system with a number of resonant peaks can be thought of as a cascade of several second order resonators.

$$X(\omega) = \sum_{<i>} X_i(\omega).$$

In addition, it is known that $X(\omega) = |X(\omega)|e^{j\phi(\omega)}$ where $|X(\omega)|$ is the magnitude response and $\phi(\omega)$ is the phase response. Therefore, the magnitude spectrum of the whole system is a product of magnitude responses of component systems and the phase response is the sum of individual phase responses. This implies that the

group delay of the complete system as well follows the additive property [22].

$$\begin{aligned} |X(\omega)| &= \prod_{<i>} |X_i(\omega)|, \\ \phi(\omega) &= \sum_{<i>} \phi_i(\omega), \\ \tau(\omega) &= \sum_{<i>} \tau_i(\omega). \end{aligned}$$

Thus, the group delay spectrum will give sharper peaks compared to the magnitude spectrum, especially when there are near by peaks.

4.6 Estimating Area Function using the Concatenated Tube Model

The concatenated tube model is widely used to model the vocal tract in speech production, where the vocal tract is considered as a concatenation of several small lossless uniform acoustic tubes, as shown in figure 4.1.

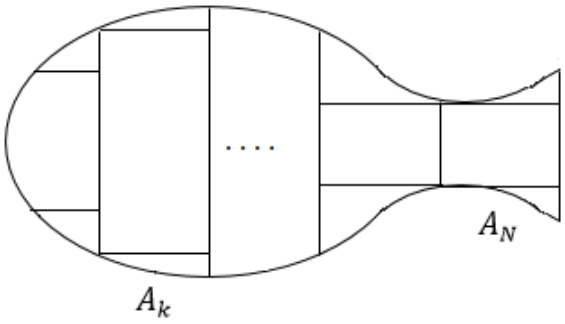


Figure 4.1: The concatenated tube model of vocal tract. Adapted from [20].

Because of the cross-sectional area changes, there will be reflection of sound wave whenever it crosses a junction between two tubelets. The reflection coefficients depends on the areas of the adjacent tubelets as, [20]

$$r_k = \frac{A_{k+1} - A_k}{A_{k+1} + A_k}, \tag{4.15}$$

where r_k is the reflection coefficient between the k^{th} and $(k+1)^{th}$ tubelets and A_k is the area of the k^{th} tubelet. These reflection coefficients are related to the partial

correlation coefficients obtained in the Levinson recursion [20] as,

$$r_i = -k_i. \tag{4.16}$$

Therefore, equation (4.15) gives,

$$\begin{aligned} \frac{1+r_k}{1-r_k} &= \frac{A_{k+1}}{A_k}, \\ \Rightarrow \frac{1-a_k}{1+a_k} &= \frac{A_{k+1}}{A_k}. \end{aligned}$$

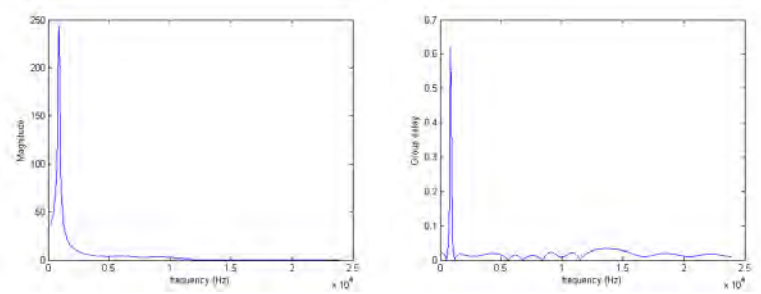
Using this equation, if the area at one of the ends of the acoustic tube (vocal tract in this case) is known, the cross-sectional area of all tubes can be found [20].

$$A_{k-1} = A_k \frac{1+a_k}{1-a_k}. \tag{4.17}$$

The relation between reflection coefficients and partial correlation coefficients (and hence LPCs) implies that the number of tubelets in the concatenated tube model decides the number of poles in the estimated spectrum. Therefore, the number of LPCs should be more for modelling a system with more resonances. The reflection coefficients are in turn related to the cross-sectional area variations. Thus, it can be inferred that the varying nature of cross-section of a system is responsible for increasing the number of resonant peaks in its spectrum.

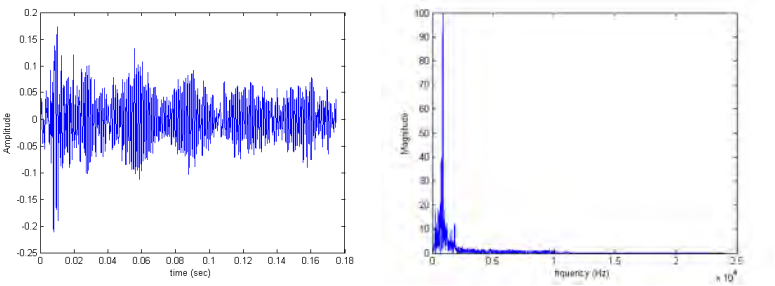
4.7 Experimental Results

LP analysis was done on columns of the Veena pillar. The LP spectrum and group delay spectrum for one column are plotted in figure 4.2 and the sound used for it is plotted in figure 4.3. *16* LP coefficients were used for analysis.



(a) LP spectrum (b) Group delay spectrum

Figure 4.2: LP analysis for a column of Veena pillar.



(a) Time-domain plot (b) Spectrum

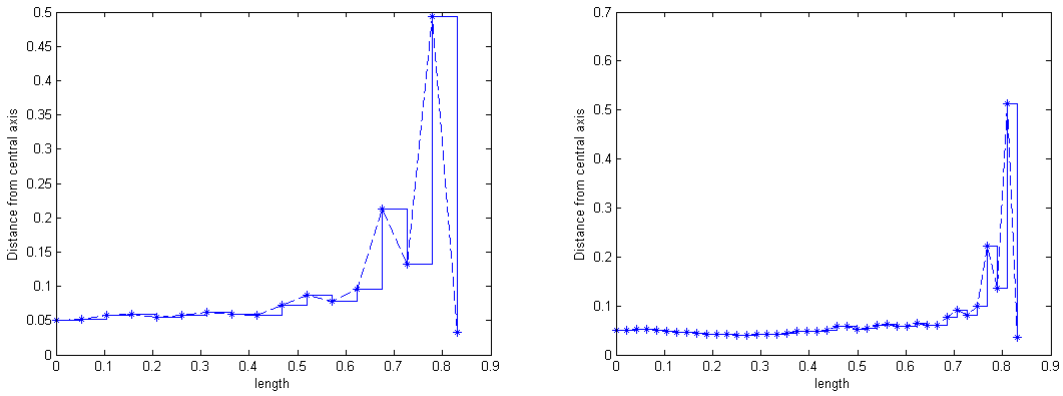
Figure 4.3: The sound from a column of Veena pillar used for LP analysis.

Comparing the results from LP analysis with the sound from pillar, it can be seen that the frequency obtained using LP analysis differs from the frequency of the sound from pillar by 5.3 %. Table 4.1 gives the numerical values of frequencies.

Table 4.1: Comparison of frequencies from LP analysis with that from pillar.

	f_1 (Hz)
LP analysis	843.7
Pillar sound	891.4

In addition to this, the area function of this musical column was also estimated. Figure 4.4 shows the distance from central axis along the length of the column for two different values of predictor coefficients.



(a) $P = 16$ (b) $P = 40$

Figure 4.4: Estimated area function for two values of prediction order.

The area function is showing an almost gradual deviation except for a sudden jump towards the end. This may be due to the connection to the pillar at the end of the column.

4.8 Chapter Summary

In this chapter, the technique of Linear Prediction (LP) was discussed and applied on the columns of musical pillar. The LP spectrum gave a close estimate of the frequency of the sound produced by the pillar. In addition, it was also possible to calculate the varying area function of the column using the concatenated tube model from speech production.

The next chapter discusses synthesis of sound from musical pillars. The method used for this purpose is the digital waveguide modelling.

CHAPTER 5
Sound Synthesis using Digital Waveguide Modelling

5.1 Introduction

Music is almost as old as the human race itself. There is a very well established link between music and mathematics. This was realized by scientists many centuries back. Theories from mathematics and physics were used to describe sound production in musical instruments.

This chapter discusses synthesis of sounds from musical pillars using digital waveguide modelling (DWG). Initially, different methods in musical sound synthesis, their advantages and disadvantages are described. The choice of digital waveguide modelling in the case of pillars is thus justified. Then the detailed theory of DWG is discussed and finally the simulation results.

5.2 Synthesis of Musical Sounds

For synthesis of musical sounds, one of the simplest and popular methods that exists is *sampling* synthesis [23]. This is nothing but the recording of the desired musical sound indexed by the control parameters which produced that sound. If an instrument is to be *sampled*, the sounds produced by all possible input combinations of the control parameters need to be recorded. It is a highly laborious task and also consumes huge storage space. Besides, the variability of control parameters is limited in case of sampling synthesis. Eventhough the results for some instruments, where the variation in control parameters is discrete (for example, struck string instruments like piano), are very impressive, this method fails for continuously controlled instruments like bowed string or wind instruments [23]. For instruments like piano, the parameter controlling the sound is the key which is pressed which is discrete. The instrument can be sampled completely if

the sounds of all the keys are recorded. However, in instruments like violin or flute, the control parameters are position of the bow, the effective length of string, pressure of blowing, amount of closure of toneholes etc., which are continuous parameters. There are an infinite number of possibilities for these parameters and hence cannot be sampled completely. One advantage of sampling synthesis is its high sound quality, which is restricted by only the recording quality.

The method discussed in the previous chapter, i.e., linear prediction is also a technique used in speech synthesis. The signal can be reconstructed using the LP residual and the LP coefficients. Eventhough the memory requirement in this method is less than that in sampling synthesis, it still has some disadvantages. It models the output sound signal and not the source. The acoustic properties of the source are not considered while modelling. This limits the quality of sound synthesized.

Another class of modelling techniques for musical instruments is *physical* modelling. It refers to the methods in which the waveform of the sound to be produced is generated using a mathematical model [24]. Such models typically have several parameters which govern the sound, which includes the constants corresponding to the material properties and dimensions of the instrument as well as the factors describing the player's interaction with the instrument (such as plucking a string or closing a tone hole) [24]. Digital waveguide modelling comes under physical modelling. Providing a mathematical model of parts of the motion within a musical instrument helps in understanding the reasons why an instrument makes the sound it does, and furthermore, how changes in shape or material affect the quality of the sound. The aim in digital waveguide modelling is to design a discrete-time model that behaves like a physical system. The theory of digital waveguide modelling has been primarily developed by Smith [25]. This technique is especially well suited to simulation of one-dimensional (*1-D*) resonators, such as a vibrating string, a narrow acoustic tube, or a thin bar. However, there exists two-dimensional and three-dimensional models ass well. DWG technique follows the physical properties of the desired acoustic system.

Digital waveguide modelling can also be used to synthesize sounds from musical pillars. The pillars produce sounds of different musical instruments which can be modelled using waveguides. The model varies for different instruments. The *1-D* digital waveguide model (which is often used to model string instruments) is discussed here in detail. The lossless *2-D* and *3-D* models are also explored to an extent.

5.3 The Ideal *1-D* Wave Equation

Consider the case of a vibrating string. The wave propagation can be considered only along the length of the string. Similarly, for the musical columns, since their length is much higher compared to their diameter, wave propagation can be considered only in one direction (along their lengths). Thus, the model used for string instruments can also be used for the musical columns. The wave equation for an ideal (lossless) vibrating string [25] is

$$Ky'' = \epsilon\ddot{y}, \tag{5.1}$$

where K is the string tension, ϵ is the linear mass density, $y(t, x)$ is the string displacement, y' is the derivative with respect to position x and $\dot{y}$ is the derivative with respect to time t. The same wave equation applies to any perfectly elastic medium which is displaced along one dimension. For example, the air column of a clarinet or organ pipe can be modelled using the *1-D* wave equation, substituting air pressure deviation for string displacement, and longitudinal volume velocity of air in the bore for transverse velocity on the string [25]. The general class of such media is referred to as one-dimensional waveguides and are used for modelling the columns of a musical pillar.

5.3.1 Travelling Wave Solution

The solution of the wave equation contains two travelling waves travelling in the opposite direction with velocity, $c = \sqrt{K/\epsilon}$. If the forward travelling wave is denoted by y^+ and the reverse travelling wave by y^-, which are arbitrary twice differentiable functions, the solution of the wave equation will be as follows [25].

$$y(t, x) = y^+(t - x/c) + y^-(t + x/c). \tag{5.2}$$

5.3.2 Sampling the Travelling Waves

To carry the travelling wave solutions to the digital domain, the travelling wave amplitudes should be sampled at intervals of T seconds. The interval depends on the required sampling rate. Accordingly, the spatial sampling interval X is the distance sound propagates in one temporal sampling interval, i.e., $X = cT$. In simulation, the wave moves left or right one spatial sample in each temporal sample. Therefore, the simulation requires only digital delay lines [25]. The change of

variables for sampling are,

$$\begin{aligned} x \to x_m &= mX, \\ t \to t_n &= nT. \end{aligned}$$

Substituting these into the travelling wave equation (equation (5.2)) gives,

$$\begin{aligned} y(t_n, x_m) &= y^+(t_n - x_m/c) + y^-(t_n + x_m/c), \\ &= y^+[(n-m)T] + y^-[(n+m)T], \\ &= y^+(n-m) + y^-(n+m). \end{aligned} \tag{5.3}$$

Since T multiplies all arguments, it is suppressed. The first term in equation (5.3) can be thought of as the output of an m sample delay line with input $y^+(n)$ and the second term as the input to an m sample delay line whose output is $y^-(n)$. The string displacement at any point in the delay line can be calculated by adding the *forward* and *reverse* travelling waves at that point [25]. An example of the ideal digital waveguide is given in figure 5.1.

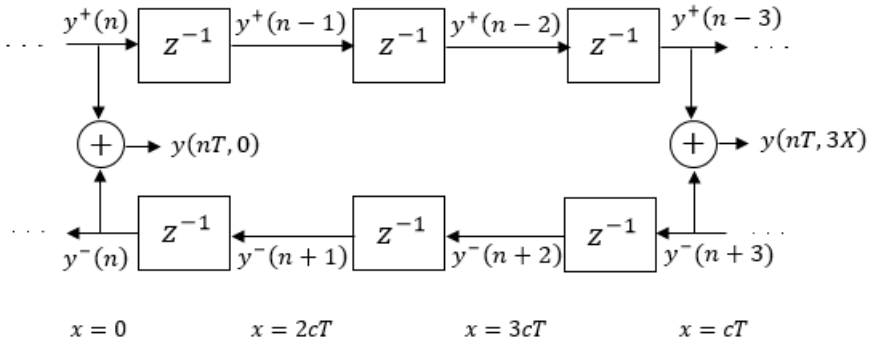


Figure 5.1: A lossless *1-D* DWG model. Adapted from [25].

5.3.3 Incorporating Losses

In any real system, there are energy losses due to various reasons. If a system like a vibrating string is considered, the losses are mainly due to yielding terminations, drag by the surrounding air and internal friction [25]. If these losses also are taken into consideration, the wave equation (equation (5.1)) will no longer be valid. Losses introduce an extra term in the wave equation [25], i.e.,

$$Ky'' = \epsilon\ddot{y} + \mu\dot{y}. \tag{5.4}$$

For small displacements, the modified travelling wave solution is obtained as,

$$y(t,x) = e^{-(\mu/2\epsilon)x/c} y^{+}(t - x/c) + e^{(\mu/2\epsilon)x/c} y^{-}(t + x/c). \tag{5.5}$$

It should be noted that both the travelling waves decay exponentially in their respective directions of travel. As done in the ideal case, the lossy travelling wave solution also is sampled with the same temporal and spatial sampling interval.

$$y(t_n, x_m) = g^m y^{+}(n - m) + g^{-}my^{-}(n + m). \tag{5.6}$$

Here, $g = e^{-(\mu T/2\epsilon)}$. The digital simulation for this lossy waveguide is shown in figure 5.2.

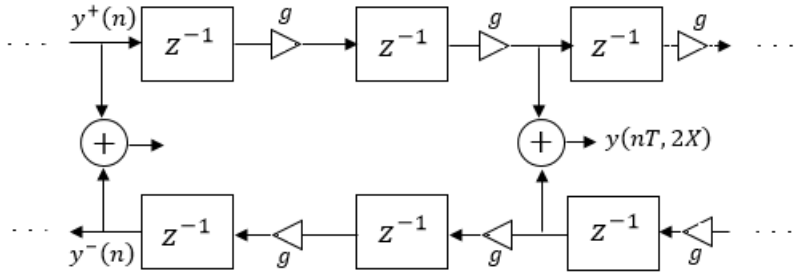


Figure 5.2: DWG model with constant loss terms. Adapted from [25].

5.3.4 Consolidating Losses

The digital simulation shown above is linear and time-invariant (LTI) and it is known that linear and time-invariant elements *commute*. Hence, the losses in the waveguide can be consolidated at one point of the waveguide for simplicity [25]. This is shown in figure 5.3. The loss factor g is pushed through delay elements until an input or output is encountered which limits the migration of loss factors.

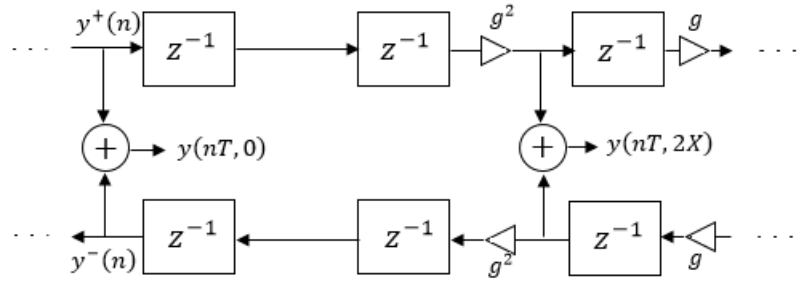


Figure 5.3: DWG model with consolidated losses, adapted from [25].

The losses can be further consolidated by pushing it through branching nodes. In that case, the loss factor in that branch should be copied to all the branches leaving the node. In addition, the inverse of the loss factor should be copied to other branches entering that node, if any.

5.3.5 Frequency-dependent Losses

In nearly all natural phenomenon, losses increase with frequency. Thus, the solution to the lossy wave equation can be generalized for a frequency-dependent case. Then, the loss factors g in the waveguide will be replaced by $G(\omega)$ [25]. These frequency-dependent loss factors can be implemented as digital filters and can be consolidated to some points as done in the case of constant losses. In addition, to avoid frequency-dependent delays, the loss filter should be a zero-phase filter. Restriction to zero-phase requires that it should be finite in length (i.e., finite impulse response (FIR) filter) and that the impulse response of the filter should be *symmetric* in time. However, this makes the filter non-causal and hence not practical. For practical purposes, it can be approximated as a causal linear-phase FIR filter [25].

5.3.6 Initial Wave Pattern

In a system modelled as a waveguide, the initial wave pattern plays an important role in deciding the final output. For example, in a lossless string model, ideally the string is plucked at exactly one point. This induces a triangular initial wave in the string, which divides into two waveforms travelling in opposite directions. However, in practice, it is not possible to pluck at only one point. Therefore, a sinusoidal wave can also be used as the initial wave pattern. Figure 5.4 shows the ideal case with triangular initial wave.

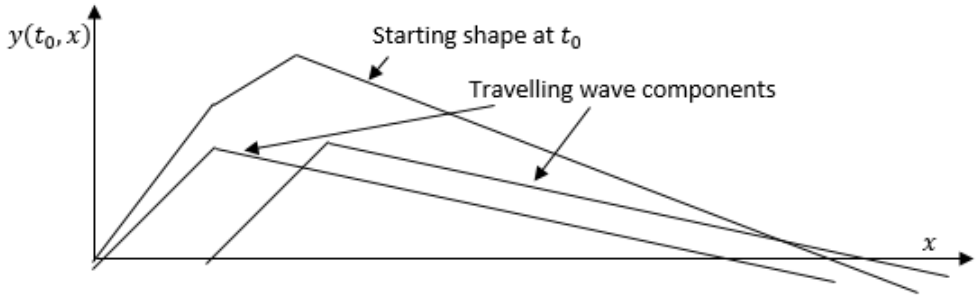


Figure 5.4: Travelling wave components in a plucked string, adapted from [25].

5.3.7 Rigid Terminations

A rigid termination is the simplest case of string termination. This implies that the string (musical column in this case) cannot move in any direction at that point. This results in the following boundary conditions [25].

$$y(t,0) = 0 \quad \text{and} \quad y(t,L) = 0. \tag{5.7}$$

These boundary conditions impose some constraints on the travelling waves which are,

$$y^+(n) = -y^-(n), \tag{5.8}$$
$$y^-(n+M) = -y^+(n-M). \tag{5.9}$$

This means that, the travelling waves are reflected completely at a rigid termination.

5.4 Towards *3-D* modelling

The extension of *1-D* waveguide to *2-D* model makes use of the concept of *scattering junctions*. The concept was introduced in [27]. Afterwards, the same was extended to *3-D* also.

5.4.1 Lossless Scattering Junctions

A scattering junction is the interconnection of several *1-D* digital waveguides [26]. Consider a junction of N waveguides. Figure 5.5 shows an example of a scattering junction and its travelling wave components.

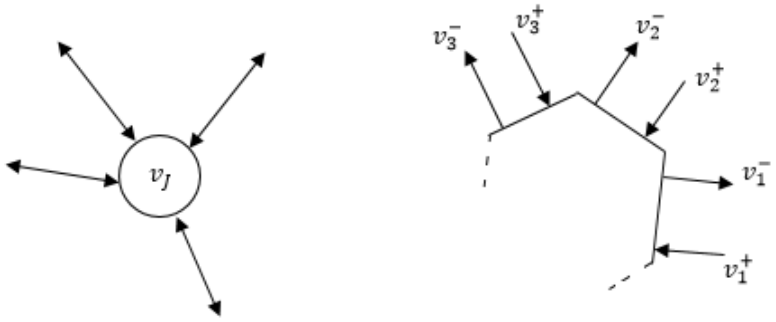


Figure 5.5: A scattering junction showing inward and outward travelling wave components. Adapted from [26].

At the junction, all waveguides must have the same velocity and all the forces must balance. If $v_1, v_2, ..., v_N$ and $f_1, f_2, ...f_N$ are the velocities and forces of each waveguide and v_J is the total junction velocity,

$$\begin{aligned} v_1 = v_2 = ... = v_N &= v_J, \quad (5.10) \\ f_1 + f_2 + ... + f_N &= 0. \quad (5.11) \end{aligned}$$

The forces and velocities of each waveguide can be resolved into left and right going components, i.e.,

$$f_i = f_i^+ + f_i^- \quad , \quad v_i = v_i^+ + v_i^-. \quad (5.12)$$

The *characteristic impedance* (Z) of a string / waveguide is defined as the ratio of force to velocity [26]. Therefore,

$$f_i^+ = Z_i v_i^+ \quad , \quad f_i^- = -Z_i v_i^-. \quad (5.13)$$

Hence, the equilibrium equation can be written as,

$$\begin{aligned} \sum_{i=1}^{N} f_i^+ + f_i^- = 0, \\ \sum_{i=1}^{N} Z_i (v_i^+ - v_i^-) = 0, \quad (5.14) \end{aligned}$$

and consequently,

$$\begin{aligned} v_J \sum_{i=1}^{N} Z_i &= \sum_{i=1}^{N} Z_i v_i^+ + \sum_{i=1}^{N} Z_i v_i^-, \\ \Rightarrow v_J &= 2 \frac{\sum_{i=1}^{N} v_i^+}{\sum_{i=1}^{N} Z_i}. \quad (5.15) \end{aligned}$$

This is the standard equation for junction velocity [26]. Assuming that all the branches have same impedance,

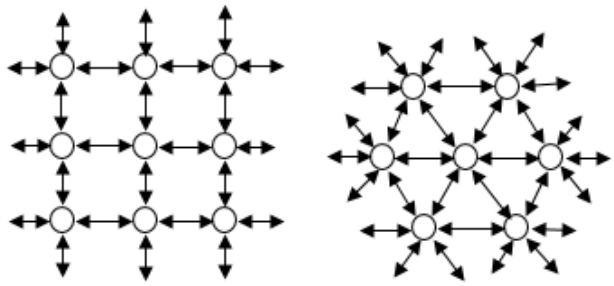
$$v_J = \frac{2}{N} \sum_{i=1}^{N} v_i^+. \quad (5.16)$$

An alternative equation can be obtained using the outgoing waves in equation

5.15.

$$\Rightarrow v_J = 2\frac{\sum_{i=1}^{N} v_i^-}{\sum_{i=1}^{N} Z_i}. \tag{5.17}$$

If different unit length waveguides are connected via scattering junctions in a particular geometry, digital waveguide meshes are obtained. Two such geometries are the *square* mesh and the *triangular* mesh. The square mesh requires *4*-port junctions while the triangular mesh requires *6*-port junctions [26]. Figure 5.6 shows these two mesh structures.



(a) Rectangular mesh (b) Tetrahedral mesh

Figure 5.6: Major *2-D* mesh structures. Adapted from [26].

As in the case of *2-D*, there are different mesh structures possible for *3-D* structures also like the *3-D rectilinear* mesh and the *dodecahedral* mesh [26]. In both these cases, the junction pressures at different scattering junctions is modelled in terms of the left and right travelling wave pressures. The rectilinear mesh is the direct extension of the square mesh in *2-D*. It requires *6*-port scattering junctions to be arranged in integer valued spatial positions along the three axial directions. The dodecahedral mesh requires *12*-port scattering junctions arranged in the *3-D* mesh, in which, each horizontal plane is a triangular mesh [26].

In the case of both *2-D* and *3-D* modelling, the number of junctions in each direction is decided by the dimensions of the system to be modelled. The boundary conditions also should be known in order to decide the reflections at the boundaries of the mesh. The simplest method is using *rimguides*, which are 1-D waveguides which connect the outermost mesh points to the boundary and bring back the signal with an inversion due to reflection [26]. The amount of reflection varies with the nature of the boundary.

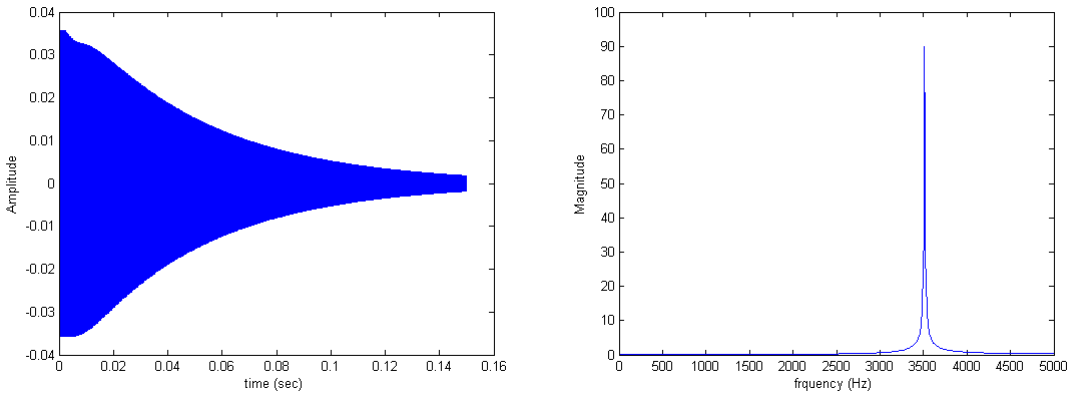
While modelling the columns of a musical pillar, the *3-D* model can be used instead of the *1-D* model. Since it takes all three dimensions of the column into consideration, it may give better results. The boundaries at the top and bottom of

the columns are attached to the pillar. Hence, complete reflection can be assumed in those cases. At other mesh boundaries, reflection occurs, but with a lower coefficient.

5.5 Simulation

5.5.1 *1-D* model

The simulation of the digital waveguide was done in *MATLAB*. The implementation was done for a lossy waveguide with frequency-dependent losses which are consolidated at one end and with rigid terminations. An example of the result is shown in figure 5.7. This particular result is for the length corresponding to *column 1* of the Veena pillar with FIR filter coefficients $\{0.5\,,\,0.5\}$ and initial plucking position at half the length of the waveguide.



(a) Time-domain plot

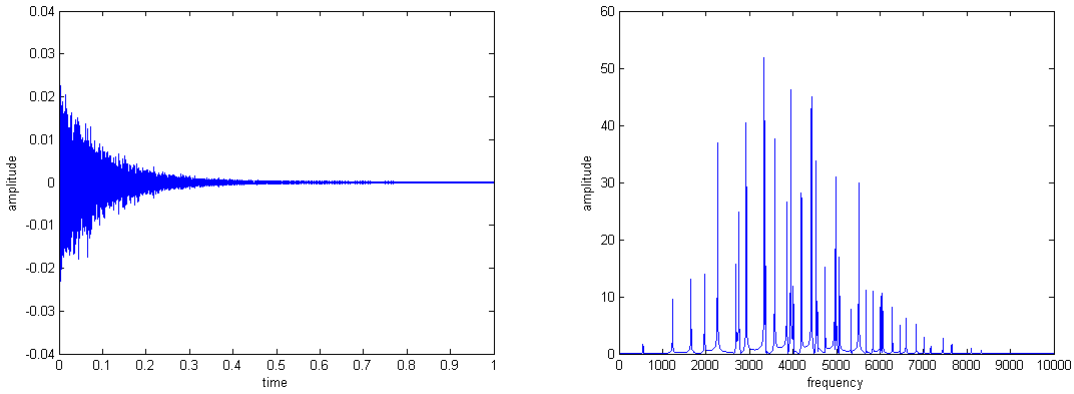
(b) correspoding spectrum

Figure 5.7: Sound synthesized using *1-D* DWG.

From the figure 5.7, it is observed that the sound produced has maximum amplitude at the beginning which decays almost exponentially with time. This damped sinusoid characteristics is matching with the sound generated by musical pillars. However, the spectrum of the sound shows a resonance peak at around $3\,kHz$ which does not agree with the measured frequency from columns. This might be because of not taking the material properties into consideration to estimate the loss filter coefficients.

5.5.2 *2-D* model

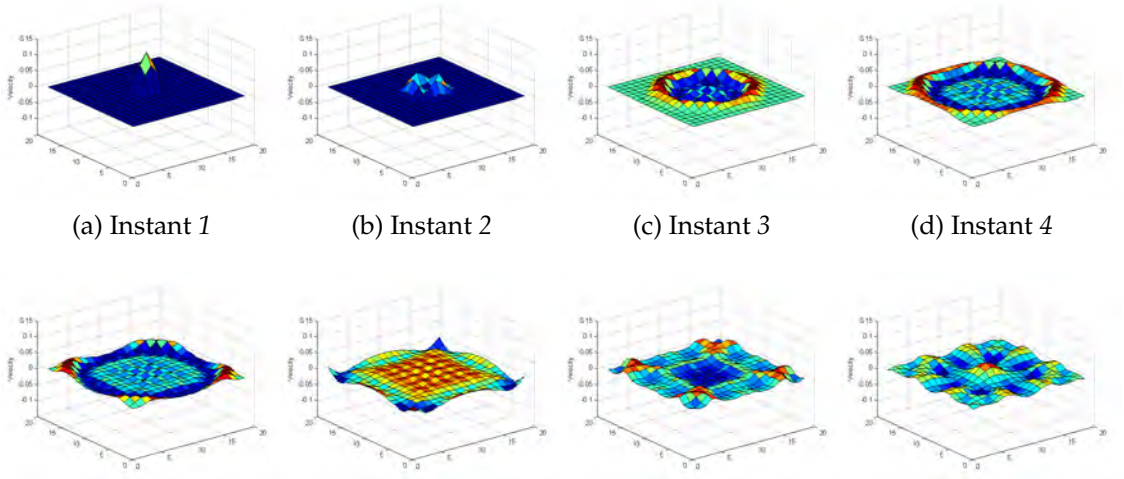
A *2-D* waveguide model using square mesh geometry was implemented for a square grid (with *20* junctions in both directions). The plot of resulting sound is shown in figure 5.8.



(a) Time-domain plot (b) corresponding spectrum

Figure 5.8: Sound synthesized using *2-D* DWG

The velocity profile of the mesh at different instants of time are given in figure 5.9.



(a) Instant *1* (b) Instant *2* (c) Instant *3* (d) Instant *4*

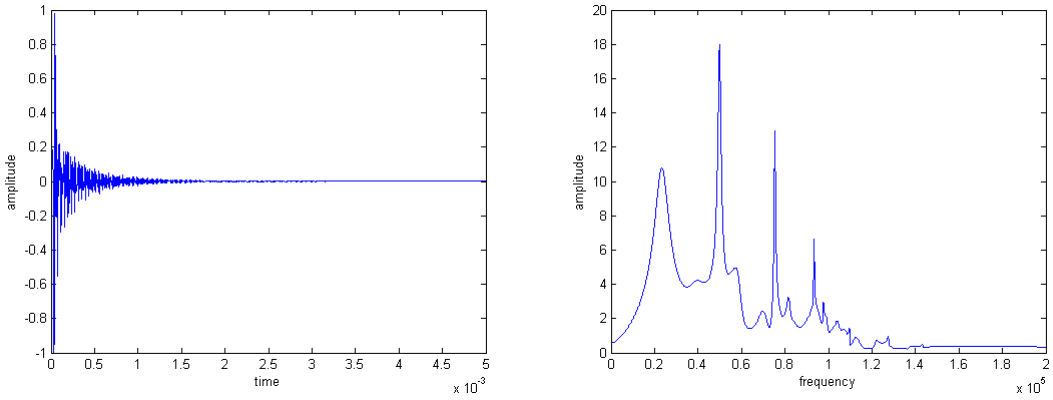
(e) Instant *5* (f) Instant *6* (g) Instant *7* (h) Instant *8*

Figure 5.9: Velocity profile of the mesh at different time instants in order.

5.5.3 *3-D* model

The *3-D* digital waveguide was implemented for the columns of the pillar producing Veena sound. A rectilinear mesh geometry was used. The number of scat-

tering junctions were calculated according to the dimensions of the columns as given in table 2.1. The number also depends on the desired sampling frequency of the synthesized sound. The plots for one particular case for *column 1* of the pillar is shown in figure 5.10.



(a) Time-domain plot (b) corresponding spectrum

Figure 5.10: Sound synthesized using *3-D* DWG

It is to be noted that in *2-D* and *3-D* waveguide models, only the losses at boundaries are considered. Internal losses due to the material properties of the columns are ignored. This will reflect in the results as well. Spectrum matching is not obtained using these models.

5.6 Chapter Summary

In this chapter, an attempt on synthesis of sound from columns of a musical pillar was made by modelling them as digital waveguides. From the *1-D* wave equation, the lossless model was obtained. Then, losses were also incorporated in the model. The *2-D* and *3-D* lossless models were discussed further and implemented. Examples of synthesized sound were also shown. However, the use of DWG for synthesizing sound from pillars was not successful as expected. The synthesized sound was not similar to the sound from the pillar.

The next chapter concludes the work done as part of this thesis and also lays out a path for future researchers to continue this work.

CHAPTER 6
Conclusions and Future Work

In chapters 1 to 5, a detailed study of the musical pillars of Vitthala temple was done. The analysis was not confined to a specific area. It covered dimensional, spectral, vibrational, signal processing and synthesis aspects of the columns and the sounds produced by them. The methods used for each of these analyses were also given in detail. This final chapter concludes the discussions and also points out some directions for future work in this area.

6.1 Conclusions from the Thesis Work

The initial portion of the thesis gave a brief history and importance of the Vitthala temple and its musical pillars. The historical structures also presented some scientific issues that needs attention. Then a detailed account of the dimensional and spectral characteristics of these pillars was given.

In beam modelling, the Euler-Bernoulli model and Timoshenko model was taken up for calculating vibration frequency. Since Timoshenko model considers some effects which are neglected by Euler-Bernoulli model, the assumption was that it will give *better correlation* with the measured frequency. However, the results got by experiments were contradicting this. The conclusion that can be made is that some other factors are causing the difference between calculated and measured frequencies rather than the *shear* and *rotation* effects of the columns. There are some common assumptions which are made while deriving both Euler-Bernoulli and Timoshenko models (Refer section 3.2). While some of these assumptions seem to be true for the columns, others are contradicting with the actual facts. This might be the reason for the deviation of theoretical values from the measured values.

Linear prediction (LP) analysis of the sound from musical pillars was also explored. The concept was taken from speech processing. Since both the vocal tract and the columns of pillars are acoustic tubes, those concepts could be applied in

the present study as well. The LP spectrum obtained showed a peak at almost the same frequency as that of the sound from pillar. The area function also was estimated using the concept of concatenated tube model.

In sound synthesis using waveguide model, a trial was done to synthesize a waveguide model for the musical columns of Veena pillar. *1-D*, *2-D* and *3-D* models were discussed. As a whole, the attempt of DWG modelling remained unsuccessful. It should be noted that the frequency dependence of material properties were not taken into consideration during synthesis. The frequency of the synthesized sound is *not* matching with that of the sound from pillar.

6.2 Future Research Directions

Scientific study of musical pillars of Vitthala temple was started only very recently. Although there has been a thorough study on flexural frequency estimation of musical columns, the synthesis techniques and spectral analysis are still in its early stages of study. There are a whole lot of other signal processing aspects of the system (i.e., musical column) and its sound which is to be analysed in detail. Next two sections list out some of the important directions for future researchers to pursue.

6.2.1 Acoustics of Musical Pillars

Vibrational analysis for frequency calculation was the most important part of all studies on musical pillars till now, including this thesis. Mainly two beam modelling techniques, *viz.*, Euler-Bernoulli and Timoshenko, have been tried till now. As per theory, Euler-Bernoulli is the simplest of all beam models whereas Timoshenko is the most complex and recent one. Therefore, the scope for future work in this area is limited or rather it is not much relevant now. However, the effect of load due to the structures on top of the columns on the vibration frequency is not studied till now. The musical columns are not isolated structures. They are connected to the pillars at both ends which are connected to other structures in the temple. They can influence the flexural frequency of the columns.

It is known that the columns of the pillar produces audible sound with as much small amount of pressure as that of a striking thumb. These sounds are correlated to the sounds of musical instruments and they are different for different pillars as well. Every stone structure of the same size and shape as that of the columns cannot produce such loud sound by just striking with a finger. Generally, in musical instruments, the sound produced by the source is amplified by

a resonating cavity. However, the pillars do not have any visible cavities. The loud sound from pillars implies that they have very low *driving point impedance*. A detailed analysis in this aspect will be very much relevant.

6.2.2 Waveguide Modelling

Eventhough *1-D*, *2-D* and *3-D* models were used for synthesizing sound from pillar, the properties of the material of construction of pillars could not be incorporated in any of the models. In *1-D* model, a loss filter was used. However, the filter coefficients were taken randomly. In *2-D* and *3-D* models, the frequency dependent losses were ignored while synthesizing. Therefore, any further study in this field must include these aspects of the models and try to achieve better correlation of frequencies of sounds from model and from pillar.

References

[1] D.Devakunjari, "*Hampi*", 2^{nd} ed., The Director General, Archaeological Survey of India, New Delhi, pp. 63-67, 1983.

[2] Anish Kumar, T.Jayakumar, C.Babu Rao, Govind K. Sharma, K.V.Rajkumar and Baldev Raj, "Nondestructive characterization of musical pillars of Mahamandapam of Vitthala temple at Hampi,India", *Journal of Acoustical Society of America*, vol. 124, no. 2, pp. 911-917, 2008.

[3] Hemant A. Patil and Shrishail S Gajbhar, "*Acoustical analysis of musical pillars of great stage of Vitthala temple at Hampi, India*", Proceedings of International Conference on Signal Processing and Communication (SPCOM), Bangalore, pp. 282-286, 2012.

[4] Acoustics, http://en.wikipedia.org/wiki/Acoustics, { Last Accessed: June 2014 }.

[5] Nondestructive testing, http://en.wikipedia.org/wiki/Nondestructive_testing, { Last Accessed: May 2014 }

[6] Saraswati Veena, pedia.desibantu.com, { Last Accessed: June 2014 }

[7] Parts of a Veena, http://www.india-instruments.com/encyclopedia-saraswati-vina.html, { Last Accessed: June 2014 }

[8] N. H. Fletcher and T. D. Rossing, *The Physics of Musical Instruments*, 2^{nd} ed., Springer, pp. 58-60, 1998.

[9] M. Karjalainen, V. Valimaki and P. A. A. Esquef, "*Efficient Modelling and Synthesis of bell-like sounds*", Proceedings of the fifth international conference on Digital Audio Effects (DAFx-02), Hamburg, Germany, pp. 181-186, 2002.

[10] Seon M. Han, Haym Benaroya and Timothy Wei, "Dynamics of transversely vibrating beams", *Journal of Sound and Vibration*, vol. 225, no. 5, pp. 935-988, 1999.

[11] Timoshenko S. P, "On the correction for shear of the differential equation for transverse vibrations of prismatic bars", *Philosophical Magazine*, vol. 41, no. 6, pp. 742-746, 1921.

[12] S.P. Timoshenko, D. H. Young, W Weaver Jr., *Vibration Problems in Engineering*, Wiley, New York, pp. 331-348, 1974.

[13] Timoshenko S. P., "On the transverse vibrations of bars of uniform cross section". *Philosophical Magazine*, vol. 43, no. 6, pp. 125-131, 1922.

[14] Erwin Kreyszig, *Advanced Engineering Mathematics*, 8^{th} ed., John Wiley and Sons Inc., pp. 46-121, 2001.

[15] Leszek Majkut, "Free and Forced Vibrations of Timoshenko beams described by single difference equation", *Journal of Theoretical and Applied Mechanics*, vol. 47, no. 1, pp. 193-210, 2009.

[16] Egor P.Popov, *Engineering Mechanics of Solids*, Pearson Education, pp. 277-292, 1998.

[17] Properties of materials, http://web.mit.edu/course/3/3.11/www/modules/props.pdf, {Last Accessed: December 2013}.

[18] Shear correction factor, http://en.wikipedia.org/wiki/Timoshenko_beam_theory, {Last Accessed: December 2013}.

[19] B. S. Atal and S. L. Hanauer, "Speech Analysis and synthesis by linear prediction of speech wave", *Journal of Acoustical Society of America*, vol. 50, no. 2, pp. 637-655, 1971.

[20] T. F. Quatieri, *Discrete-Time Speech Signal Processing Principles and Practice*, Pearson Education, pp. 136-200, 2002.

[21] M. H. Hayes, *Statistical Digital Signal Processing and Modelling*, John Wiley & Sons, pp. 215-268, 1996.

[22] B. Yegnanarayana and Hema A. Murthy, Significance of Group Delay Functions in Spectrum Estimation, *IEEE Transactions on Signal Processing*, vol. 40, no. 9, pp. 2281-2289, 1992.

[23] J.O. Smith, Physical Audio Signal Processing, http://ccrma.stanford.edu/~jos/pasp/, online book, 2010, {Last Accessed: February 2014}.

[24] Physical modelling, http://en.wikipedia.org/wiki/Physical_modelling_synthesis, {Last Accessed: April 2014}.

[25] J. O. Smith, "Physical modelling using digital waveguides". *Computer Music Journal*, vol. 16, no. 4, pp. 74-91, 1992.

[26] Marc Laurent Aird, "*Musical Instrument modelling using digital waveguides*", Ph.D. Thesis, University of Bath, United Kingdom, pp. 1-50, 2002.

[27] S. A. Van Duyne and J. O. Smith III, "*Physical Modeling with the 2-D Digital Waveguide Mesh*", Proceedings of the International Computer Music Conference, ICMC-93, pp. 40-47, Tokyo, 1993.

[28] Mathematica user guide, http://reference.wolfram.com/mathematica/guide/Mathematica.html, {Last Accessed: March 2014}.

[29] Temple bell sound, https://www.youtube.com/watch?v=bvBwuC7ZgMI, {Last Accessed June 2014}.

APPENDIX A
Basic Definitions from Mechanics

A.1 Elasticity

Elasticity is the property of a material by which an internal force opposes the external force and brings it to its original shape after it is deformed. An object's tendency to be deformed elastically is called as *elastic moduli*. It is a measure of resistance of the material to external force. There are various elastic moduli like Young's modulus, Shear modulus and Bulk modulus.

A.2 Young's Modulus and Hooke's Law

Young's modulus is a measure of stiffness of a material. It is defined as the ratio of stress (with dimensions of pressure) to strain (dimensionless) over the range of stress values for which Hooke's law holds. It is the most popular elastic moduli eventhough there are other moduli like the bulk modulus and the shear modulus.

The Hooke's law states that the force F needed to compress/extend a spring by a distance x is proportional to that distance, i.e.,

$$F = kx,$$

where k is the spring constant. Hooke's law is also satisfied to some extent by elastic bodies when they are deformed.

A.3 Shear in Beams

To maintain a segment of a beam in equilibrium (If the whole beam is in equilibrium, then any segment of it should also be in equilibrium), there must be an internal vertical force V at the ends so that vertical forces are cancelled. This internal force acting at right angles to the beam is called shear. It is numerically equal

to the sum of all vertical components of external forces acting on the isolated segment but opposite in direction.

Shear modulus or modulus of rigidity is the elastic moduli concerned with deformation due to shear forces. It is mathematically expressed as the ratio of shear stress to shear strain.

A.4 Bending Moment in Beams

For attaining moment equilibrium, there should be internal resisting moment within the cross sectional area of element to counteract the moment caused by external forces. These moments tend to bend the beam and are hence called as bending moments.

A.5 Radius of Gyration

Radius of gyration is a measure of the size of an object which is calculated as the root mean square distance of the parts of the object from its center of gravity. The two dimensional Radius of gyration describes the distribution of the cross sectional area of a column around its central axis.

A.6 Poisson's Ratio

When a body is compressed in one direction, it tends to expand in the other two directions perpendicular to the direction of compression. This is called as the Poisson effect and a measure of this is the Poisson's ratio. It is the ratio of the percentage of expansion to the fraction of compression.

A.7 Moment of Inertia

The area moment of inertia also known as the second moment of area is a geometrical property of an area which shows the distribution of its points with respect to an arbitrary axis. It is different for different shapes of area.

APPENDIX B
Important MATLAB Codes

B.1 LP analysis

```
%---Finding LP spectrum---%
[signal,fs]=wavread('veena1.wav'); % Reading file
P=16;         % Prediction order
len=length(signal);
signal_fft = fft(signal,2^nextpow2(length(signal)-1));
auto_corr = ifft(abs(signal_fft).^2); % autocorrelation
auto_corr = auto_corr./len;       %  idft of power spectrum.
[LPCs,e,k]=levinson(auto_corr,P);      % Finding LPCs
sig_residual=filter([0 LPCs],1,signal); % LP residual
[LP_spec,w]=freqz(1,[0 LPCs]);      % LP spectrum
LP_phase=phase(LP_spec);
LP_groupdelay=abs(diff(LP_phase));  % group delay spectrum
%---Finding area function---%
len_column=0.83;           % Length of the column
len_segment=len_column/P;   % Length of one tubelet
len_x_axis=0:len_segment:len_column;
Diameter_col=0.10186;      % Diameter of the column
radius_col=Diameter_col/2;
area_now=pi*radius_col^2;  % Area at one end
area_array=area_now;     % Initializing area function
ref_coeff=-k;   % partial correlation coefficients
ratio_k=(1-ref_coeff)./(1+ref_coeff);  % (1-rk)/(1+rk)
N=length(ratio_k);
for i=0:N-1
    area_next=area_now*ratio_k(end-i);  % Area of next tubelet
    area_array=[area_array area_next];  % Updating area function
    area_now=area_next;
end
```

B.2 *1-D* DWG

```
%initializations
len_actual=0.84;  %length of the column
d=15000;  %No. of samples
x=0.5;  % plucking position
c=5300;  %velocity
t_del=0.00001;  %temporal sampling interval
x_del=c*t_del;  %spatial interval
delays=floor(len_actual/x_del);  %No.of delays
left=zeros(1,delays);    %backward wave
right=zeros(1,delays+1);  %forward wave
pickup=delays;  % output pickup point
pl_pos=x*(delays-1);
% initial wave shape
shape = [[0:floor(pl_pos)]/pl_pos,(delays - 1 -
        [(floor(pl_pos)+1):(delays-1)])/(delays
        - 1 - pl_pos) ];
left=shape/2;
right(1:delays)=shape/2;
y=zeros(1,d);  % output variable
%wave propagation in loop
for i=1:d
  left = [left(2:delays),0];
  nut = -left(1);  % rigid termination
  right = [nut, right(1:delays)];
  bridge = -(0.5*right(end)+0.5*right(end-1)); %loss filter
  left(delays) = bridge;
  y(i) = left(pickup) + right(pickup);

end
```

B.3 *2-D* DWG

```
N = 30000;  %No. of samples
fs = 22050;  %playback sampling rate
N_jn = 20;  %No. of junctions
% Initialize calculation matrices.
%forward and backward waves in x,y,z directions.
vxp = zeros(N_jn,N_jn); vxm = zeros(N_jn,N_jn);
vyp = zeros(N_jn,N_jn); vym = zeros(N_jn,N_jn);
vxp1 = zeros(N_jn,N_jn); vxm1 = zeros(N_jn,N_jn);
vyp1 = zeros(N_jn,N_jn); vym1 = zeros(N_jn,N_jn);
v = zeros(N_jn-1,N_jn-1);  %velocity profile
```

```
y = zeros(1,N);  %output variable
% Provide initial velocity profile
dim = floor(N_jn/5);
start = floor((N_jn-dim)/2);
vals = zeros(N_jn-1,1);
vals(start:start+dim-1) = 0.25*sin(pi*[0:dim-1]/(dim));
valm = vals*transpose(vals);
vxp1(1:N_jn-1,1:N_jn-1) = valm; vyp1(1:N_jn-1,1:N_jn-1) = valm;
vxm1(1:N_jn-1,2:N_jn) = valm; vym1(2:N_jn,1:N_jn-1) = valm;
%wave propagation in loop
for n = 1:N,
  if ( mod(n,2) == 0 ), % tick0
    v = 0.5 * (vxp(1:NJ-1,1:NJ-1) + vxm(1:NJ-1,2:NJ) +
               vyp(1:NJ-1,1:NJ-1) + vym(2:NJ,1:NJ-1));
    % Update outgoing junction wave components.
    vxp1(1:N_jn-1,2:N_jn) = v - vxm(1:N_jn-1,2:N_jn);
    vyp1(2:N_jn,1:N_jn-1) = v - vym(2:N_jn,1:N_jn-1);
    vxm1(1:N_jn-1,1:N_jn-1) = v - vxp(1:N_jn-1,1:N_jn-1);
    vym1(1:N_jn-1,1:N_jn-1) = v - vyp(1:N_jn-1,1:N_jn-1);
    % Do boundary reflections.
    vxp1(1:N_jn-1,1) = -0.99*vxm(1:N_jn-1,1);
    vxm1(1:N_jn-1,N_jn) = -0.99*vxp(1:N_jn-1,N_jn);
    vyp1(1,1:N_jn-1) = -0.99*vym(1,1:N_jn-1);
    vym1(N_jn,1:N_jn-1) = -0.99*vyp(N_jn,1:N_jn-1);
  else % tick1
    v = 0.5 * (vxp1(1:NJ-1,1:NJ-1) + vxm1(1:NJ-1,2:NJ) +
               vyp1(1:NJ-1,1:NJ-1) + vym1(2:NJ,1:NJ-1));
    % Update outgoing junction wave components.
    vxp(1:N_jn-1,2:N_jn) = v - vxm1(1:N_jn-1,2:N_jn);
    vyp(2:N_jn,1:N_jn-1) = v - vym1(2:N_jn,1:N_jn-1);
    vxm(1:N_jn-1,1:N_jn-1) = v - vxp1(1:N_jn-1,1:N_jn-1);
    vym(1:N_jn-1,1:N_jn-1) = v - vyp1(1:N_jn-1,1:N_jn-1);
    % Do boundary reflections.
    vxp(1:N_jn-1,1) = -0.99*vxm1(1:N_jn-1,1);
    vxm(1:N_jn-1,N_jn) = -0.99*vxp1(1:N_jn-1,N_jn);
    vyp(1,1:N_jn-1) = -0.99*vym1(1,1:N_jn-1);
    vym(N_jn,1:N_jn-1) = -0.99*vyp1(N_jn,1:N_jn-1);
  end
   % Do output calculation.
  y(n) = v(N_jn-1,N_jn-1);
end
```